Multi-scale Modeling and Simulation of Nanoparticles Reinforced Polymer Composites

A Thesis

Presented to the

Graduate Faculty of the

University of Louisiana at Lafayette

In Partial Fulfillment of the

Requirements for the Degree

Master of Science

Xiaoguang Xiao

Spring 2018

Multi-scale Modeling and Simulation of Nanoparticles Reinforced Polymer Composites

Xiaoguang Xiao

APPROVED:

Ahmed Khattab, Chair Associate Professor of Industrial Technology	Mohammad Jamal Khattak Professor of Civil Engineering
Peng Yin Assistant Professor of Mechanical Engineering	Pengfei Zhang Assistant Professor of Industrial Technology
Mary Farmer-Kaiser Dean of the Graduate School	

ACKNOWLEDGMENTS

I am grateful for all the help from all the great people I met in my graduate life. They not only inspired me during my research, but also in my daily life.

First of all, I would like to express my gratitude to my advisor, Dr. Ahmed Khattab, for being such a great leader in this lab. He has always been so generous in helping me with my research and sharing his life experience with me. He cares not only about his students' academic performance, but also their lives. From the very beginning I barely knew how to do research independently, and I credit Dr. Khattab's correct guidance for the development of that skill. Throughout the last two years, he has been guiding me with patience and enthusiasm, making lab research very enjoyable. I am so honored to have him both as my teacher and my mentor in life. His academic input and financial support makes my thesis work possible, which is greatly appreciated.

I would like to acknowledge Dr. Mohammad J. Khattak for generously offering his time and giving me advice and direction so that I could stay on the right track. He has always pointed out problems in my research accurately. Further, this acknowledgment cannot be complete without thanking my Ph.D. advisor, Dr. Peng Yin, who has provided me opportunities to go further in mechanical engineering. Moreover, Dr. Pengfei Zhang gave me a lot of previous advice about how to do research, and I want to express my gratitude to him. As a student, I am honored to learn from such esteemed faculty members. Also, I would like to thank every one of my class instructors at the University of Louisiana at Lafayette.

In addition, I would like to thank my research group members Baobao Tang, Dijon Hill, Roger Johnson, Blake G. Dexter, and Shuosheng Luo for their help in my research.

I would like to thank my parents, Mr. Jianhan Xiao and Mrs. Jinfeng Li, my younger brother, Zhixue Xiao, and all my friends for their love and constant support. Their inspiration has kept me devoted to my studies.

TABLE OF CONTENTS

LIST OF TABLES

LIST OF FIGURES

LIST OF ABBREVIATIONS

ALE	Lagrangian and arbitrary Eulerian
CNF	Carbon nano fibers
CNT	Carbon nano tubes
EISA	Evaporation-induced self-assembly approach
FEA	Finite element analysis
HDPE	High-density polyethylene
LDPE	Low-density polyethylene
MWNT	Multi-walled nano tubes
PB	Polybutadiene
PET	Poly- (ethylene terephthalate)
POMMs	Periodically organized mesoporous materials
PP	Polypropylene
PP/CNT	Carbon nano tubes reinforced polypropylene composite material
PS	Polystyrene
PVC	Polyvinyl chloride
RTM	Resin transfer molding
RVE	Representative volume element
VGCNF	Vapor-grown carbon nano tubes

INTRODUCTION

Problem Statement

Polymer has been widely applied in aerospace, automobiles, sporting goods, and other areas. It is well-known for being durable, strong, lightweight, and reasonable in price when compared with conventional materials. In the last 20 years, the development of advanced technology has been thriving. People expect even better mechanical properties in materials, which stimulates more in-depth researches on polymer materials[1]. Researchers found that mechanical properties of polymer composites can be improved significantly by adding a small amount of inclusion, such as fibers, whiskers, and particles. Moreover, those small amounts of inclusions do not influence weight and ductility very much. However, not satisfied with the advancement of materials brought by the microparticles, people are seeking a breakthrough on using smaller particle sizes.

Nowadays, Nanoparticle-reinforced composite materials have been capturing a lot of attention. It has been found that nanoparticles influence effective mechanical properties significantly in many ways, such as increasing energy absorbing capability during impact and improving toughening effect[2–6]. The rapidly developed electronic technologies give more exposure to the atomic structure of nanoparticles, such as scanning electron microscopy, scanning force, and laser scanning laser fluorescence. Those technologies provide more opportunities for people to investigate the influence of particle size and weight percentage on mechanical properties[7]. Experiments show that nanoparticles have a remarkable contribution to material mechanical and electronic properties. Usually, particles with a dimension range from 1 to 100 nm are defined as nanoparticles.

Great endeavors have been made by researchers to process customized composites and conduct experiments on them. With those achievements, a new generation of researchers have access to works related to the theory, preparation, and characterization of various types of nanocomposites[8–11]. However, making personalized materials is very time-consuming, since the state-of-art composite materials are usually not price-friendly, which makes progress within a short period challenging. This issue now is being solved by taking an approach to the computational modeling using finite element analysis software. Continuum mechanics theory contributed significantly to the finite element analysis, which simplifies the modeling process while successfully predicts the overall mechanical properties of the materials. Using the continuum mechanics theory on models in [2, 12–15] have validated that the computational models at nano or micro scale can agree with the experimental results very well if models are built properly. Researchers now face two major problems simulating composite materials at the nano and micro scale due to the following two reasons: firstly, it is not realistic to build a macro model that contains hundreds and thousands of nanoparticles under standard laboratory conditions. Secondly, the time needed to solve the model increases exponentially with the complexity of a model. Attempts have been made by Y. Liu [16] using supercomputer JITSU PRIMEPOWER HPC2500, which has 128 CPUs, to conduct a simulation on a model embedded with 2000 carbon fibers. However, this modeling condition is not achievable in most of computational laboratories due to limited computer processing power. The current models built for simulation of composite materials in most of research are either focusing on one scale or a single type of material. That is also why little research has been done to bridge the connection between nanoscale, microscale, and macroscale.

Current micromechanical properties are dependent on the fact that effective mechanical properties are functions of properties of components and interfaces, which is widely applied to the prediction of mechanical properties of composite materials. The nanoscale model serves as a foundation for microscale and macroscale during the simulation process, and it is crucial to choose the mechanical parameters wisely for nanoscale models in order to keep micro and macro models consistent. Microscale models are mainly constrained by the number of basic unit models employed and computer processing capability, which also brings more restrictions to model design. Except for some tests on supercomputers, not much research has been conducted at a macro scale until now. Regarding macroscale research on nanoparticle reinforced composites, the advanced experimental techniques and equipment allow materials to be thoroughly investigated on overall mechanical properties. However, the correlation between computational simulation and preliminary tests remains to be built. Even though several attempts have been made to model carbon nanotubes (CNT), massive nanoscale models and high requirements for computer CPUs become the major hurdles on the way of further research[17].

In this research, based upon the Law of Mixture, a methodology is proposed by using representative models to simulate nanoscale particles reinforced composites and further extended to microscale models. verification of models is conducted on CFR materials.

Goal and Objectives

The goal of this project is to present a generalized methodology of studying nanoparticles reinforced polymer composites, which helps the simulation of mechanical properties through multiscale finite element modeling approach while being less time-demanding and labor-intense. With this methodology, the gap will be bridged between thoroughly investigated

overall mechanical properties under the experimental condition and scarce of investigation on the behavior of materials at the nanoscale. To achieve the goal of this study, several sub-objectives will be completed, which are listed below:

(1) Construct a general nanoscale unit model for polymer nanocomposites and conduct a computational study to examine the tensile behavior of the model at nanoscale using FEA-based LS-DYNA software.

(2) Validate the nanoscale unit model by comparing the simulation result with the published data.

(3) Conduct a sensitivity study on the nanoscale models with various mesh sizes to optimize the mesh size with respect to computational time and model accuracy.

(4) Construct multiple models at microscale featured with various nanoparticles reinforcement weight percentages and orientation using optimized unit models.

(5) Determine the sensitivity of nanoparticles dosage and their orientation effects on the mechanical properties of the component materials using developed microscale model.

(6) Validate the developed microscale model by comparing the simulation results with published experimental data.

During the research, knowledge of strain, stress, Young's modulus, Poisson's ratio, and the physical relationship between each other will be employed. To guarantee the minimum error that occurs in statistics processing, statistical analysis software JMP 11 will be in cooperation with LS-DYNA.

Research Methodology

This research is non-experimental since it focuses on providing a methodology to bridge the gap between nanoscale simulation and macroscale simulation on nanoparticles reinforced polymer composites. The entire computational work contains three main parts to help to validate models: modeling, simulation, and mathematical analysis.

In the modeling part: At the nanoscale, a general unit model is developed on LS-Prepost beforehand, which includes a unit of the nanoparticles and a unit of the polymer matrix. There are several factors to be used to define the unit model: the dimension, mechanical properties of components, mesh size. The dimension and mechanical properties of a model are determined according to the weight percentage of nanoparticles and measured mechanical properties of nanocomposites in the reference experimental research. At micro and macro scale, the unit models are stacked in specific orders to make a square shape, and the interface among unit models are defined based on the mechanical properties of the matrix. According to the arrangement direction of the nanoparticles, the loads are applied to faces of the nanocomposite models to examine the effects of arrangement direction on effective mechanical properties.

In the simulation part, all the models are simulated on LS-DYNA solver. Regarding the double precision is very time-demanding, single-precision setting is used throughout the entire simulation work. D3PLOT file is output to view the tensile simulation process. Memory size is set as the maximum in case that the computers cannot solve the complex models.

In the mathematical analysis part, the models are assumed to be isotropic material and obey the Hook's Law when the materials are deformed in the elastic region. The continuum theory is applied to calculate the Poisson's ratio and Young's modulus.

This methodology applies all the three major parts to each of scale: nanoscale, microscale, macroscale. The flowchart of the methodology is shown in Figure 1. This flowchart provides a visual illustration of how the models are constructed, simulated, and validated.

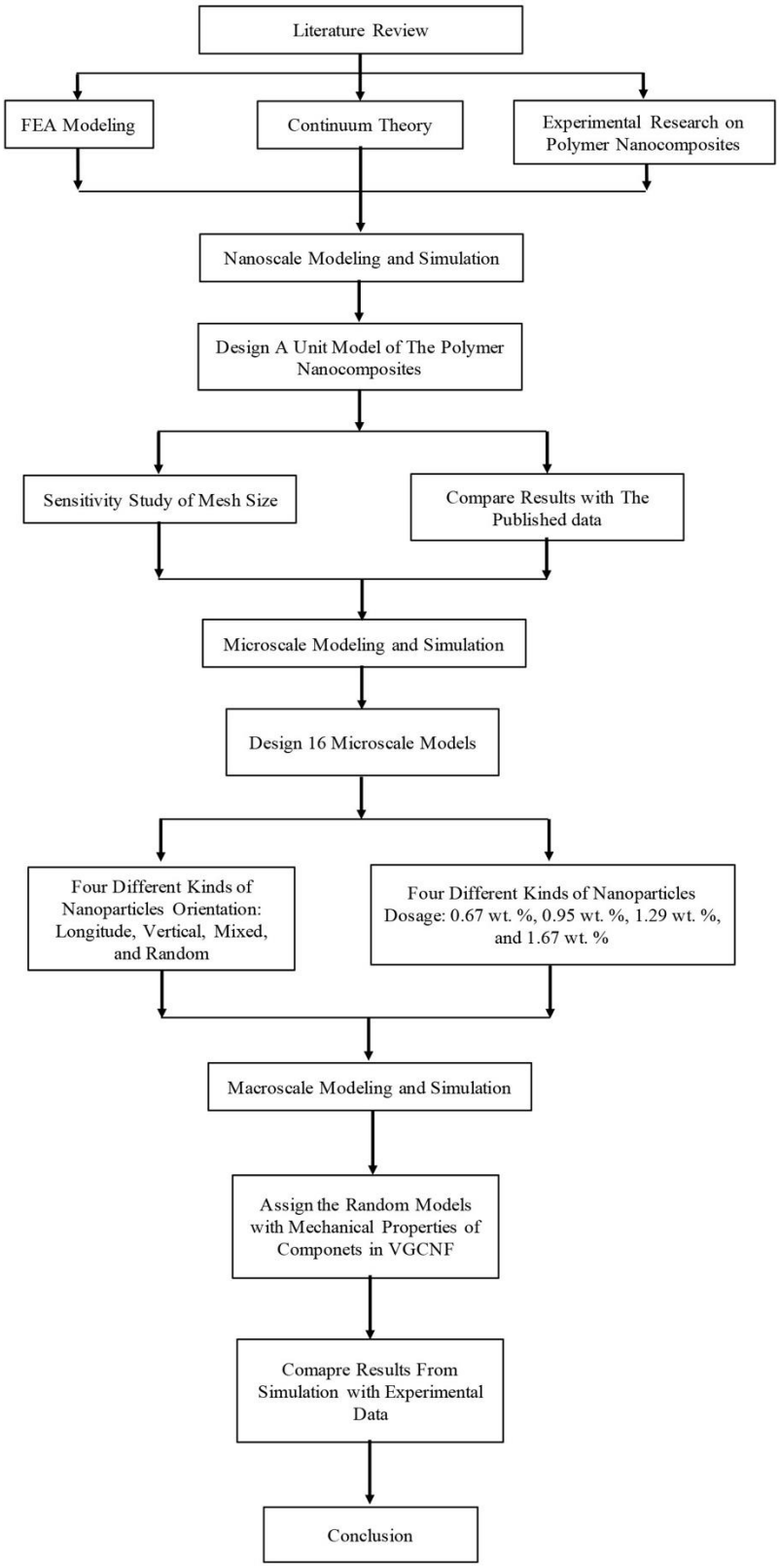

Figure 1. A flowchart of the research methodology.

CHAPTER I: LITERATURE REVIEW

Composite Materials

Reinforced composite materials have existed in human history for thousands of years. For example, ancient Egyptians (1500 B.C.) built reinforcing mud walls with bamboo shoots and laminated wood. Concrete as another composite material has been in human history since the pre-Roman period[18], and research on the cistern of Kameiro-Rhodes (500 B.C.) show that pozzolanic concrete is covering the walls of the reservoir [19]. The development of processing technology accelerates the creation of varying composite materials. In the 20th century, the modern composite materials started showing up, such as glass fiber reinforced resins, which was widely applied to boats and aircraft. Since the 1970s, people have sought more advanced materials to guarantee safety and performance in harsher working environments, which spurred the development of techniques that produced new fibers such as carbon, boron, and aramids, along with new composite systems with matrices such as metal and ceramics[19]. Constituent materials in traditional composites, which focuses mainly on the improvement of overall mechanical properties regardless of weight-to-strength ratio, are usually abundant in quantity and easily accessible. Composite materials are defined as materials comprised of two or more constituent materials that feature significantly different physical or chemical properties but produce superior overall properties than any of the individuals. Matrix and reinforcement are two major components in the composite material; matrix helps bond fillers together, transfer loads between fillers, and protect the fibers from the environmental attacks such as chemical erosion, abrasion, and moisture. while the reinforcement helps to improve the capability of carrying a load, and an appropriately chosen reinforcement could increase the capability massively; the reinforcement may be in the form

of particles, flakes, fibers, or chunks. According to the types of matrix phase, composites can be cataloged into metal matrix composites, ceramic matrix composites, and polymer matrix composites. The classifications on the basis of reinforcement are classified into particulate composites, fibrous composites, and laminate and sandwich structure composites as shown in Figure 2 [20].

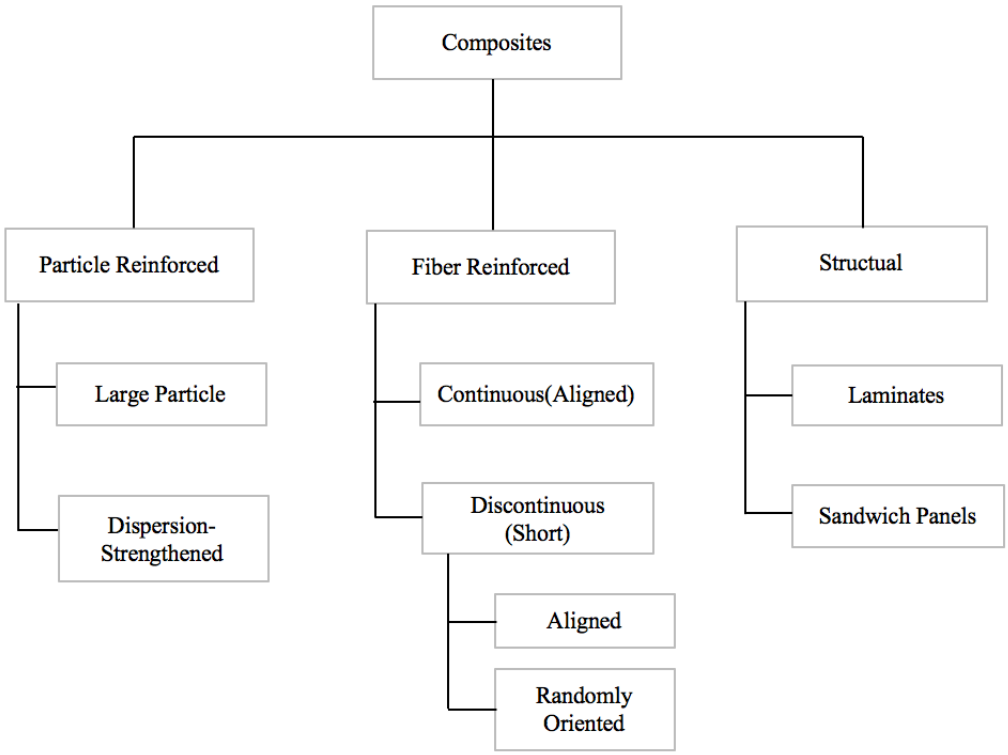

Figure 2. Composite materials structural chart.

The composite material, on the basis of its formation, can be classified into naturally formed composites and artificial composites. Artificial composites include all the composite materials that are human-made. Natural composites are materials such as wood, where the lignin matrix is reinforced with cellulose fibers, and human teeth, which consist of enamel and dentin. Advanced materials, which are a type of artificial materials were initially utilized in the aerospace industries, these materials, such as carbon fiber/epoxy, Kevlar/epoxy, and

boron aluminum composites, feature high performance and low mass density. Compared with traditional composites, advanced composites are more competitive in mechanical properties. Also, advanced composites were more expensive especially decades ago when mass production of advanced composites was still very challenging. Nowadays, most advanced materials are not inaccessible to ordinary people. Advanced composite materials such as carbon fiber/resin have extended their utilization to skateboards or bicycles. Advanced composite materials are advantageous over traditional materials in several ways, which include strength, stiffness, fatigue and impact resistance, thermal conductivity, and corrosion resistance, etc.[18]

The matrix in composites is a homogeneous and monolithic material that provides binding and protection for reinforcing materials such as fibers, particles, or whiskers from environmental and physical damage. The matrix contributes significantly to the mechanical properties of a composite material. A material can be a matrix in composites if it can provide:

1. The feature that soaks reinforcement at a temperature that will cause melting, thermal degradation or structural disorientation reinforcement.
2. The chemical property that lacks reaction between matrix and reinforcement.
3. Continuity of a uniform matrix distribution that can reach up to 60-65 percent volume over the whole interstitial spaces.

There are three kinds of matrices that are widely used in industry: metal, ceramics, and polymers. Metal matrices can provide electrical conductivity, ductility, and high stiffness. Usually, alloys of aluminum, magnesium, and titanium are preferable when designing a material that requires lightweight and excellent mechanical properties. Ceramics are advantageous when the application environment is at high temperatures, and ceramic matrix

materials are featured with oxidation and corrosion resistance, high strength, and stiffness. However, ceramics are brittle and hard to process. Nowadays, technology can use reinforcing metals such as aluminum to make ceramic materials less brittle. Polymer is the most widely used and preferable matrix in industry. Polymer matrix composite materials have high specific strength and specific modulus, excellent fatigue resistance and high damage tolerance, and also superior damping characteristics. Moreover, processing polymer matrix materials are more accessible than processing metal and ceramics.

Application of Composite Materials

Applications of composite materials mainly focus on aerospace industry and other more typical industries for economic purpose. Even though the application of composite materials on the aerospace area is a small portion, in regards of guaranteeing safety and best performance in extreme working environment, it represents the most advanced technology in this area. For instance, the maiden flight of The French Rafale (1980), consisted of 50% advanced composite materials in its wings, vertical and the fuselage structure. For the United States B-2 stealth bomber (1989), advanced composite materials contributed to 40% of its body structure. Also, the utilization of advanced composite materials in the modern helicopter has upwards of 50% to 80%. The multi-mission, tiltrotor military aircraft, which is capable of conducting vertical takeoff and landing, and short takeoff and landing, uses 3 tons of composite materials, which accounts for 45% of the total structural weight. Besides the military reasons, advanced materials are also extensively employed on commercial airplanes as statistics demonstrate. The approximate usage of composite materials in the Boeing B707 is 18.5 m^2, the B737 is 330 m^2, and the B747 is 930 m^2, during a 10-year span, the use of composite materials has increased ten times of the usage in the very beginning[21]. There are

small aircrafts that entirely use composite materials in their structure; the Voyager, fully equipped with composite materials, broke the world record with its 9-day non-fuel and non-stop trip.

In addition to aerospace, the applications of composite materials are everywhere in our daily life. Composite materials have been applied in the transports for over a half century, such as vehicles, ships, and trains. Composite materials can be used in an engine cover, dashboard, seats, and in the structural body. For the chemical liquid transportation, composite materials make it possible to transport some very active chemical products since the specially tailored composites have high corrosion resistance and lack reaction with chemical things. Composite materials also contribute significantly to electrical and electronic industries. Metals such as Cu, Au, Ag-Pd, the polymer polyimide, and ceramics such as Al2O3, AlN, and glass-ceramics can be used to make Substrate, which is a chip carrier that more chips can be attached to and an interconnection can be built on[22]. Composite materials are also used as the resistor because high electric currents pass through resistors generating a significant amount of heat. This heat causes an inverse effect on the resistance of the resistor if one applies a regular resistor. However, if polymer-matrix composite and carbon-carbon composites are applied, the resistor can perform stably at high temperatures. In the mechanical manufacturing factory, composite materials occur in the turbine blade, pumps, pipes, gears, flange, etc.

Polymer Matrix Composites

Currently, the most widely used composite materials are polymer-matrix composites (PMC), in which polymers such as epoxy, polyester, or urethane serve as the matrix and thin diameter fibers such as graphite, aramids, or boron serve as reinforcement. The polymer

includes the general plastics and rubber, which are featured with large molecular structures and in chain form. Many polymers are super ductile and pliable, which means they can be quickly reformed geometrically at a specific temperature limit without changing their chemical properties. The polymer can be divided into two classifications: homopolymers and copolymers. Home-polymers are polymers which consist of monomers of the same kind while the copolymers have different repeating units. There are some typical polymers, and their properties are demonstrated in Table 1[23].

Table 1. Common polymers.

Name	Abbreviation	Common Uses	Properties
Poly-(ethylene terephthalate)	PET	Soda Bottles	Amorphous
High-density Polyethylene	HDPE	Food Container	Crystalline, rigid
Polystyrene	PS	Styrofoam cups	Brittle
Polyvinyl chloride	PVC	Piping	Hard
Polypropylene	PP	Plastic Drinking straws	Tough, Flexible
Kevlar	Kevlar	Bullet-proof vests	Stronger than steel
Polybutadiene	PB	Automobile Tires	Flexible, soft

The mechanical properties of PMC mainly depend on the leverage between polymer and fibers. Unlike the ceramic composites using the reinforcement to improve its toughness, polymer matrix composites are designed to use reinforcement to support main mechanical loads that the structure is subjected to. Polymer matrix composites are usually classified into two categories: reinforced plastics and advanced composite materials. Reinforced plastics

have a very economical price and are reinforced with low-stiffness glass fibers. The mechanical properties of polymer composite materials can be affected by several factors: 1. Interfacial Adhesion, which is defined as the binding between a reinforced element and polymer matrix. The binding can be at the molecular scale which is achieved by chemical reaction or physical absorption. The extent of binding determines the mechanical properties, and current technology has been able to provide an insight investigation on the interface at the atomic level by using tools such as the atomic force microscopy (AFM) and nano-indentation devices. 2. Shape and orientation of dispersed reinforcement. Particles that have preferred direction could affect the properties significantly; even though, it might be simply used for improving mechanical properties or to lower the cost of isotropic materials. For example, Md. A Bhuiyan et al.'s modeling reveals that carbon nanotubes orientation affects the tensile modulus up to 8%[24]. 3. Matrix Properties. The type of polymer matrix determines the application of PMC, and thermoplastic polymers consist of linear or chained-like molecular structures that have weak intermolecular bonds. Polymers such as such as polyethylene, polycarbonate, and nylon can be re-shaped by melting them at a specific temperature or by applying a force. Another kind of polymer is thermosetting, which features cross-linked or network structures with covalent bonds with all molecules. This kind of polymer is not re-shapeable.

New Technology and New Composite Materials

More advanced technology has been achieved to improve designing and preparation methods of composite materials, such as gradient compositing. The gradient compositing causes the mechanical properties to distribute in a gradient way based on the loads the material is subjected to. Gradient composite materials are tailored to be more economical while

maintaining excellent performance. Some other technologies such as self-spreading, molecular self-assembly, and super-molecular compositing are also very widely used now. Conventionally, composite molding is the primary way to manufacture composite components. An example of this is resin transfer molding (RTM), which has been employed since the 1990s. Melted thermosetting resin, mixed with fibers, are injected into a closed mold and then solidified with heat until it is ready. RTM is advantageous with its single equipment, short molding time, and most importantly excellent performance.

A new technology that comes into our view is the hybrid materials, which are generally described as the mixture of inorganic and organic components. Nowadays, the coverage of this term has been broadened to include micro-particles and nanoparticle with their increasing use. The applications of hybrid composite materials are extensively related to many areas: 1. Mesostructured thin films periodically organized mesoporous materials (POMMs) based upon their intrinsic characteristics can be used for sensors, fuel cells, etc. The new evaporation-induced self-assembly approach (EISA) makes it possible to design micro- or nanopatterns on a film. 2. Lego-like hybrids, a strategy used to incorporate the inorganic nano-objects into an organic polymer matrix. Through this approach, properties of the material such as the mechanical, gas barrier, electrical insulation, and flame incapability can be improved. 3. Hybrids for energy, hybrid materials have great potential to combine desirable components to tailor the mechanical and transport properties of batteries with nano-blocks. 4. Commercial applications. Hybrid materials can be used on automobile parts, decorative coatings, sealants, dental products, etc. The SCHOTT company developed a glass that is specifically for oven baking trays and has a distinctive transparent lens which is easy-

to-clean because of the functional hydrophobic siloxanes embedded in an organic network layer[5].

Nanocomposite Materials

The manufacturing and application of polymers in aerospace, automobiles, and sporting goods have been ubiquitous since it is durable, strong, light-weight, and price reasonable when compared with conventional materials. Traditional composite materials are usually reinforced with microparticles, which are defined as having a length between 0.1 and 100 micrometers. Recent processing techniques are capable of producing nano-sized particles at high purity. A large number of experimental research has proved that a small amount of inclusions can contribute to material mechanical properties phenomenally. Current micromechanical theories are employed based on the idea that the effective properties, such as Young's modulus, of the composite material are affected by the volume fraction, mechanical properties, and arrangements of inclusions. However, these theories might not be correct if applied to nanomaterials. In the last 20 years, the thriving development of advanced technology with higher and stricter requirements on mechanical properties spurred further research on polymer materials[1].It is found that a small amount of inclusion, such as fibers, whiskers, and particles in polymers, could improve the mechanical performance significantly while maintaining the light-weight and ductile properties. After a few years of application of micro-sized reinforcements, processing technologies have been developed for the employment of processing advanced materials that are reinforced with nanoparticles. Experiments show that nanoparticles have made an extraordinary contribution to material mechanical and electronic properties.

Nanocomposite materials are those materials whose size ranges from 1 nm to 100 nm. Because of the unique characteristics of nanocomposites, a reduction in size without change in substance materials can improve properties such as electrical conductivity and insulation, elasticity, higher strength, etc. Nanocomposites have attracted constant attention due to the fact that when the dimension of the reinforcement reaches the nanoscale, the properties of composites are affected significantly by nano-filler dispersion, dimensions, arrangement direction, volume fraction, and the interfacial properties between filler and matrix[25]. The rapidly developed electronic technologies, such as scanning electron microscopy, scanning force, and laser scanning laser fluorescence, enable the revealing of the atomic structure of nanoparticles, which has spurred research on the influence of particle size and weight percentage on mechanical properties. Geometrical size has been the major hurdle of modeling composite materials, with regards to reducing the computational work while maintaining the accuracy. Gaurav Nilakantan incorporated a method called Hybrid Element Analysis (HEA) on the flexible woven fabric, which features both 3D solid model and 2D shell model[26]. To further decrease the computational requirements, the fabric models are designed in a gradient way so that the level of modeling resolution decreases with distance away from the impact center. This demonstrates a good agreement of results between the HEA approach and a baseline fabric model. Gusev proposed a method using spherical representative volume element to simulate composites based upon the knowledge that composites are heterogeneous locally while behaving homogeneously in sufficiently large samples[27]. To implement the Monte Carlo(MC) realizations, they placed a required number of spheres on a cubic lattice inside the unit cell. The elastic constants were investigated on a periodic elastic composite with disordered cells that contained randomly

distributed 8, 27, and 64 non-overlapping identical spheres, the results revealed that the scatter of individual estimates were practically stationary when compared with the average elastic constants obtained from varying numbers of spheres. Gusev's research laid a foundation for studying fracture micromechanics of composite material. K. Hbaieb et al. compared two-dimensional finite element studies to a three-dimensional model. Based upon the simulation results on the nearly aligned and randomly oriented nano-clay particles, the Mori-Tanaka model exhibits a reasonably accurate prediction of the stiffness of clay nanocomposites when the volume fraction is less than 5%. However, it underestimates the stiffness at higher volume fractions in 3D FEM. Even though some researchers have used 2D models to approximate the mechanical properties of composite materials, it was proved in K. Hbaieb's simulation that 2D demonstrations are consistently lower than 3D models while both 2D and 3D models exhibit lower stiffness than actual material stiffness[28].

Nanoparticles reinforced Polymer Composites

Nowadays, other than the consideration of better mechanical properties, people expect much more from materials, such as high strength-to-weight ratio, which is already beyond the traditional materials' capability. When particles are at nano size, the main characteristics are focused on the surface. The surface energy produced by large surface to volume ratio on nanoparticles aggregates particles to generate a larger size. However, if the aggregation is prevented properly, the nano-sized individuals are maintained and exhibit a quantum-size effect, macro-quantum effect, tunnel effect, surface effect and interface effect, which are summarized as nano-effects. These effects help the material produce excellent mechanical, electrical, and optical properties[21]. Research on properties of nanocomposites has been going on for decades. In the early 1990s, it is reported that Toyota Central Research

Laboratories in Japan found that a small percentage of nano is capable of boosting the thermal and mechanical properties significantly[29].

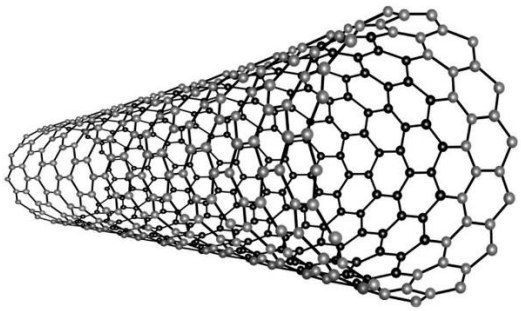

Figure 3. Carbon nanotube model.

Currently, the research on nanoparticles demonstrates its potential to make a significant enhancement of mechanical and electrical properties of composites. Increasing yields from research reveal exceptionally superior mechanical, electrical and thermal properties of nanoparticles such as carbon nanotubes (CNT) (as shown in Figure 3) and carbon nanofibers (CNF) [29, 30]. Especially when employed as reinforcing material in composites, nanoparticles attract enormous attention with their capability to improve mechanical properties significantly by adding a small amount. Zhang et al. [31]studied impact behavior of PP/CNTs containing one wt.% with two different lengths of CNTs. They found that toughening effects of nanotubes highly depended on testing temperature. Xiao et al. [32]investigated the low-velocity impact and tensile behaviors of PP/CNT nanocomposites. Both tensile strength and impact resistance were found to increase when the CNT content reached 0.6 wt.%. These improvements in mechanical properties are all related to uniform dispersion of nanotubes prepared by shear mixing. Mahdieh M Zamani et al.[4]studied the polymer nanocomposites containing 0.75, 1.0 and 1.5 wt.% of multi-walled carbon nanotubes (MWNTs) in a polypropylene (PP) matrix in relation to their low and high-velocity impact

performances. Results showed better ballistic limit velocity (the average of highest impact velocity causing perforation but unable to go through and lowest impact velocities with no residual velocity recording) and higher energy absorption for specimens, each containing 1 wt.% MWNT. When studying on the low-density polyethylene (LDPE) composites reinforced with vapor-grown carbon nanofibers (VGCNF), Ahmed Khattab et al. found that the strength and Young's modulus of VGCNF/LDPE composites were improved by 15% and 44% respectively when increasing the VGCNF to 3wt%.

Finite Elements Analysis

Finite element analysis (FEA) is a computational technique that is used to obtain approximate solutions of boundary value problems and is mainly utilized in the simulation of structures where continuum mechanics are applicable[33]. The approximation of solutions is developed based on Taylor's series, and the FEA method has been evolving during the last few decades. The traditional finite element method requires additional approximation when it comes to the boundary conditions of gradient type. In addition, the very early finite difference formulas were developed using the triangle grids. Owing to the improvement on the traditional FEA, now the grids are not limited to one shape. Grids also might vary in one FEA model as shown in Figure 4.

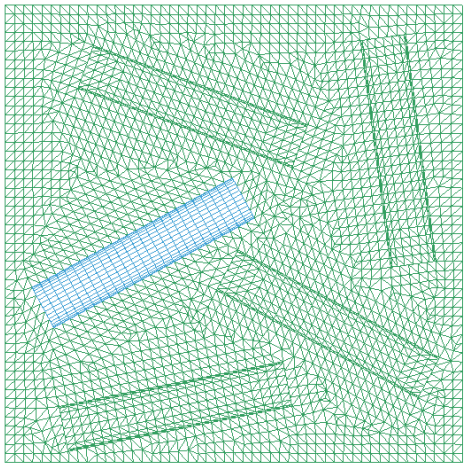

Figure 4. An example of FEA model with various grid sizes.

In FEM, there are three formulations that have been widely used: Eulerian, Lagrangian, and Arbitrary Lagrangian Eulerian (ALE) methods. In terms of the broad application of FEA methods, a significant amount of research is abundantly available with regards to the numerical analysis of the performance on the laminated composites under different types of loads. (X.L Chen and Y.J. Liu developed a method with which the carbon nanotubes were built as continuum structure instead of an atomic structure on ABAQUS. The results show that the simulation is consistent with those from the experiments. Yijun Liu et al. also utilized ABAQUS to study the local load transfer, interface properties and failure modes at the nanoscale, in which carbon nanotubes were treated as continuum fibers in the elastic matrix. This showed high potential for large-scale modeling. Another technique LS-DYNA also widely employed to gain a complete understanding of how nanoparticles microscopically govern the overall impact and penetration behavior. LS-DYNA is a program dealing with the real-world problem with adequately designed finite elements (FE). By conducting a simulation on LS-DYNA, a connection is built between the microscopic changes in CNTs and observable, overall impact behavior of the nanocomposite through

multiscale models. In this pilot study, an ideal case is assumed for the FEA models, where perfect CNT/PP contact and individually dispersed CNTs are considered (no interphase, no agglomerates). The RVE used in the FEA and proposed impact simulation are considered the perfect alignment of the CNTs along the loading direction. In the FE modeling, CNTs are assumed to be rigid rod structures. The 3D RVE with the applied boundary conditions will be investigated under uniform extension (the linear portion of the stress-strain curve) to determine the effective Young's Modulus of CNT/PP composites. A higher-order 3D structural brick element with 3 degrees of freedom per node will be used to model the material. The RVE (Representative Volume Element) model will act as a continuum substitute of the atomic CNT structure, which has been validated by X.L Chen et al. [13, 29, 34] by conducting tensile test and impacts behavior analysis. RVE in this paper is a nanocomposite unit that consists of 1.6 wt% of CNT and polypropylene by referring from the article by X.L Chen [13]. Both CNT and polypropylene are considered as homogeneous material, which means, the tensile test simulation is conducted under ideal conditions. Forces are applied in a linear elastic range, in which the elasticity theory can be applied appropriately. Some other crucial mechanical property data is derived from the paper published by M. M. Zamani et al. [35].

Modeling of the Mechanical Properties of Nanoparticles/Polymer Composites

Currently, the research on nanoparticles which has a nanoscale dimension demonstrates its potential to make a significant enhancement of mechanical and electrical properties of composites. Increasing yields from research reveal exceptionally superior mechanical, electrical and thermal properties of nanoparticles such as carbon nanotubes (CNT) and carbon nanofiber (CNF) [29, 30]. Y. Zare studied interfacial characteristics between the

matrix and nanofiller using various micromechanic models, and it was found that the shape memory polymer nanocomposites with strong interfacial adhesion between matrix and nanofiller showed very good memory properties[36]. In this researcher's later research, the nanoparticles aggregation/agglomeration in polymer composites through building simple modelings of PP/PPgMA/SiO_2 for mechanical properties, [37]. B. Mortazavi et al. conducted simulations on polymer nanoparticles to investigate the interphase (Figure 5) effects on the elastic modulus and thermal conductivity. They compared the effects of filler geometry, volume fraction, and interphase thickness on thermal conductivity and elastic modulus[38].

The basic unit for modeling is very crucial since it influences not only the accuracy of the result but also the modeling time. A. Pontefisso et al. developed a new algorithm for the generation of three-dimensional representative volume elements using the Ripley function. This function makes it easy to mesh and import the representative volume elements[39]. V. Marcadon et al. investigated the confrontation between molecular dynamics and a micromechanical approach on how particle size affects mechanical behavior of polymer nanoparticles. The simulation shows that increasing the particles radius while maintaining the volume fraction will increase the elastic moduli. However, the confrontation indicates that the interface definition will affect the elastic moduli result[40].

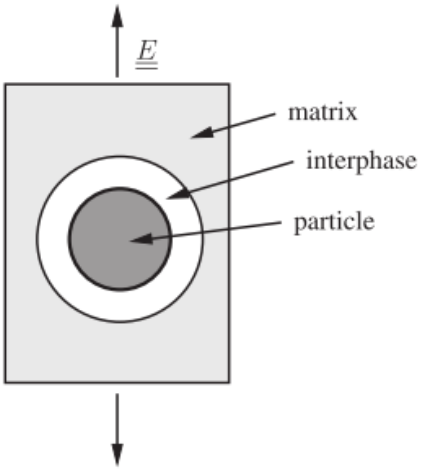

Figure 5. Assumed interphase layer in the model.

Especially when employed in reinforcing the material in composites, nanoparticles attract enormous attention with their capability to improve mechanical properties significantly by adding a small amount. [41]Y. Zare also used the Halpin-Tsai model to simulate polymer nanocomposites by assuming interphase properties and nanofiller size. It was found that the developed model can accurately predict the interphase properties by Young's Modulus. Moreover, the smallest particle size and largest interphase volume fraction make the best Young's modulus in polymer composites. [42]M. Quaresimin et al. use modeling to study the dominant damaging mechanisms as a function of filler type and describe the physics of material behavior based on the materials relevant length scale. [43] K. Jajam et al. examined the role of nano- vs micro-filler particles size-scale on static and dynamic fracture behavior on silica-filled epoxy composites. They found that the particle size-scale does not have significant influence on elastic and physical properties at a given volume fraction based on the study of volume percentage from 3% to 10%. Zhang et al. [31]studied impact behavior of PP/CNTs containing 1 wt% with two different lengths of CNTs. They found that toughening effects of nanotubes highly depended on testing temperature. Xiao et al. [32]investigated the

low-velocity impact and tensile behaviors of PP/CNT nanocomposites. Both tensile strength and impact resistance were found to increase when the CNT content reached 0.6 wt.%. These improvements in mechanical properties are all related to uniform dispersion of nanotubes prepared by shear mixing. Mahdieh M Zamani et al. [31] studied the polymer nanocomposites containing 0.75, 1.0 and 1.5 wt% of multi-walled carbon nanotubes (MWNTs) in a polypropylene (PP) matrix in relation to their low and high-velocity impact performances. Results showed better ballistic limit velocity (the average of highest impact velocity causing perforation but unable to go through and lowest impact velocities with no residual velocity recording) and higher energy absorption for specimens, each containing 1 wt% MWNT. When studying on the low-density polyethylene (LDPE) composites reinforced with vapor-grown carbon nanofibers (VGCNF), Ahmed Khattab et al. found that the strength and Young's modulus of VGCNF/LDPE composites were improved by 15% and 44% respectively when increasing the VGCNF to 3wt%.

Summary

The literature review provides a comprehensive study of the discovery, development, and improvement of composite material from the perspective of research on mechanical properties. Heretofore, nanoparticle reinforced composites have been a promising solution for researchers who are devoted to discovering materials with the high strength-to-weight ratio. The current research tendency indicates that more and more research will be conducted, which will investigate the nanoparticle reinforced materials. In regards to the fact that viewing the process of failure inside composites is not operable under microscopy, it is urgent to find a solution that could help researchers understand how micro failure mode could be related to macro-mechanical properties. Currently, computational simulations and modeling are considered as a promising solution by using the FEA concept. However, the existing hurdle at this moment is that work for the modeling and simulation of microscale models is massive. The modeling and simulation are very time-demanding and challenging to computational conditions in most laboratory. Moreover, unlike carbon fibers that arrangement could be customized at an advantage of observable size, the nanoparticles are embedded in the polymer in a random or agglomerative way, which makes it difficult to conduct experimental tests to investigate the influence of nanoparticle orientation. Once the gap between the microscale models and macroscale model is bridged, the failure mode and mechanical properties of macroscale model can be predicted at a micro scale, thus saving a lot of time and reducing the investment on experiments.

CHAPTER II: NANO AND MICRO MODELING

Nano Modeling

Model-building preparation. Simulation on an FEA model is very time-consuming. It is critical to shorten the time spent on solving a model while maintaining relatively high accuracy. Nano modeling in this research is to build a basic unit model appropriately with respect to optimize the accuracy and simulation time. There are several factors affecting the time and accuracy; mesh size is the primary factor and shape of the basic unit model is another factor. Mesh is the grid generated in the model when FEA is employed. Normally, it takes longer to generate finer grids on models. Also, the smaller the mesh size is, the longer time needs to finish solving a model. In some instances, it is accompanied by the exponential increase of simulation time even if 1% of lifting on accuracy is tried. Using basic unit models to build a larger scale model is like using Lego blocks to build a castle, unit models that are wisely chosen are helpful for obtaining better similarities to real things. However, Nanoscale particle reinforced composites contain thousands and millions of Nanoparticles, and there is no way to mesh and model them together under the current laboratory condition. In this study, an RVE is a basic unit model that contains enough statistical information to predict the mechanical properties of one kind of nanocomposites. It is designed to include the same percentage of Nanoparticles as the whole material, as shown in Figure 5. It contains a unit of polymer and a unit of nanoparticles. The size of the RVE is designed based on the average dosage of nanoparticles in nanocomposites. In order to find the balance among mesh size, computing time, and accuracy, a sensitivity study needs to be conducted on the RVE, which will be shown in detail in the following part.

Effective moduli in stress-strain relationship. Figure 6 shows a very general heterogeneous material that contains the polymer and tube-shaped fillers, each direction of this material has different mechanical properties. In order to show how this material reacts to an applied force, an interest point is assigned to a random spot on the surface of the material to do the mathematical analysis.

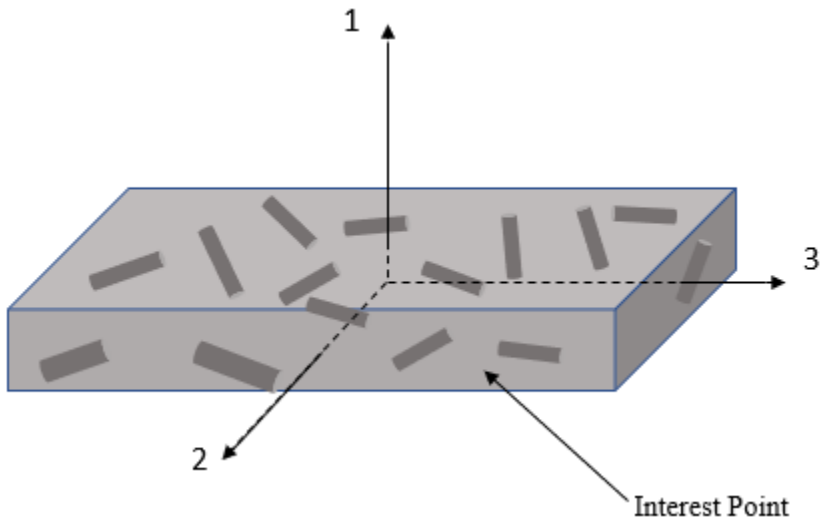

Figure 6. An example of heterogeneous material and three normal directions.

The interest point is isolated as shown in Figure 6. The cubic in Figure 7 is an imaginary point used to describe the general three-dimension stress state of a spot on the material, which is defined by nine stress components. Since the cubic is symmetric, the stresses on six faces can be simplified to 3 faces, on each face the stress is denoted as $\sigma_{ij,}$ σ_{ij} (where i, j = 1,2,3). When i=j, for example, $\sigma_{11,}$ σ_{ij} is normal stress, and when i≠j, σ_{ij} is shear stress.

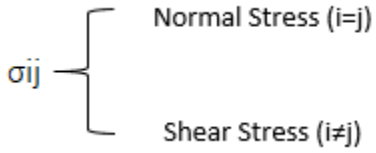

Where, i means the face on which the stress components act, j means the direction of stress components act.

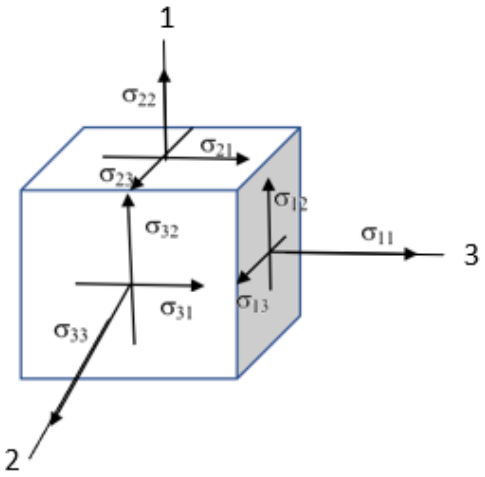

Figure 7. Normal stress on the assigned point.

Correspondingly, when force is applied to the material, the deformation will be created. The deformation at a point is described as the strain. Normal strain means the change in length along the axis direction, which is direction 1, 2, and 3 in Figure 7. Generally, the relationship between stress and strain can be expressed in a formula:

$\sigma ij = C \times \varepsilon ij$

Where: C is an elastic constant

εij is strain

For a non-homogenous material, the C is not the same during the calculation if the force is applied in the different position. The most general linear relationship between stress and strain is given in a 9x9 matrix as given below, in which [C] means the elastic moduli of this material.

$$\begin{Bmatrix} \sigma_{11} \\ \sigma_{12} \\ \sigma_{13} \\ \sigma_{21} \\ \sigma_{22} \\ \sigma_{23} \\ \sigma_{31} \\ \sigma_{32} \\ \sigma_{33} \end{Bmatrix} = \begin{bmatrix} C_{1111} & C_{1112} & C_{1113} & \cdots & C_{1133} \\ C_{1211} & C_{1212} & C_{1213} & \cdots & C_{1233} \\ C_{1311} & C_{1312} & C_{1313} & \cdots & C_{1333} \\ & & & & C_{2133} \\ & & & & C_{2233} \\ & & & & C_{2333} \\ & & & & C_{3133} \\ & & & & C_{3233} \\ C_{3311} & & \cdots & \cdots & C_{3333} \end{bmatrix} \begin{Bmatrix} \varepsilon_{11} \\ \varepsilon_{12} \\ \varepsilon_{13} \\ \varepsilon_{21} \\ \varepsilon_{22} \\ \varepsilon_{23} \\ \varepsilon_{31} \\ \varepsilon_{32} \\ \varepsilon_{33} \end{Bmatrix}$$

When research of mechanical properties was done on a point, it found out that the stress and strain are always symmetrical (i.e., $\sigma ij = \sigma ji$, $\varepsilon ij = \varepsilon ji$), which means the elastic constant matrix is symmetric with respect to the diagonal line. The possible stress distribution of a heterogeneous material on both ends is shown in Figure 6. As we can see that the stress σ1 is not equal at every spot on the surface.

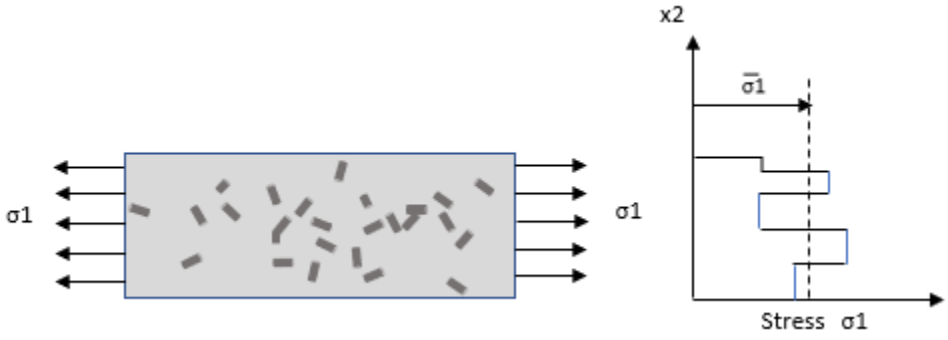

Figure 8. Heterogeneous composite under different stresses.

For a composite material as demonstrated in Figure 4 that reinforcements are at Nano-scale, the reinforcement size is even smaller than the matrix molecule, the shape and size of reinforcement can be ignored when we do the stress-strain analysis. The entire material can be treated as a homogeneous composite.

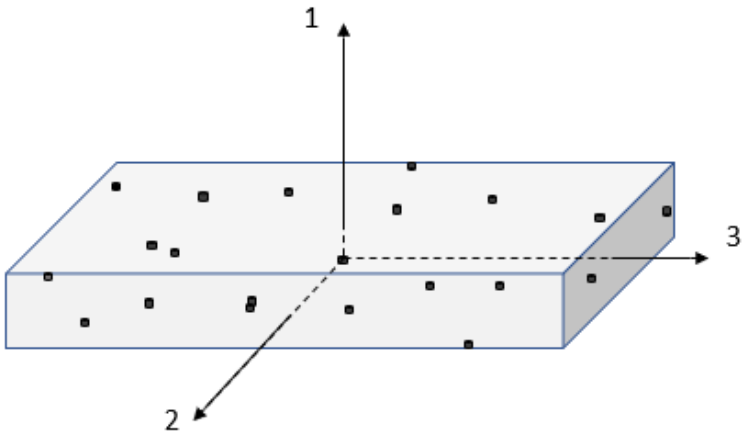

Figure 9. Nanocomposite material example.

Figure 9 depicts a composite material that matrix is the polymer (grey cubic area), and reinforcement is carbon Nanotube (black dots). Similarly, taking an interest point to do the analysis, the equivalent homogeneous material under same average stress with Figure 8 is shown in Figure 8

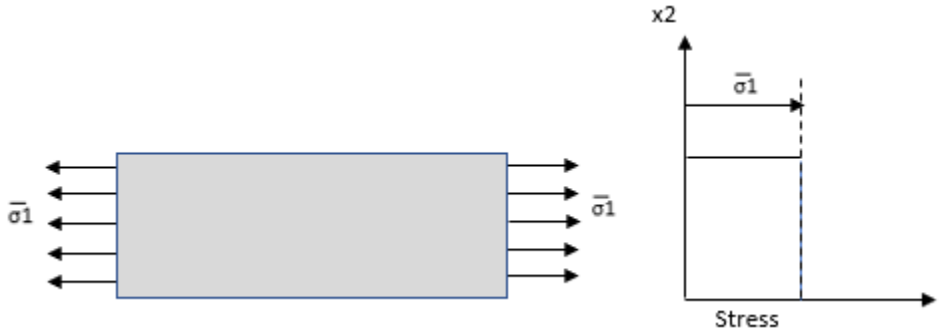

Figure 10. Equivalent homogeneous material under average stresses.

Representative volume element model. Representative Volume Element is the smallest unit of a model, which contains enough statistical mechanisms to predict the properties of a whole model. Conditions need to be satisfied to define the RVE clearly: unit cells are in a periodic microstructure and volume contains a huge set of micro-scale elements[44]. Based on the definition of RVE, the best way to design RVE for nanoparticles

reinforced composites is that each RVE contains one nanoparticle as shown in Figure 11. For illustration purpose, Carbon nanotubes reinforced polypropylene is chosen to design a qualified RVE.

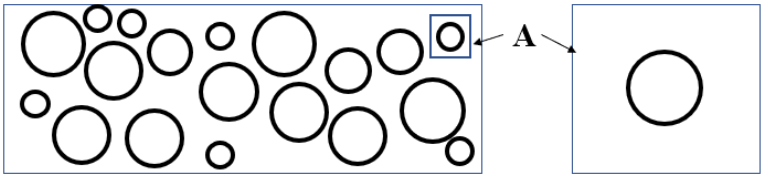

Figure 11. A is an RVE example from the material.

A qualified representative volume element should be proper in size and can convey the fundamental information of the entire material. To build a similar structure of PP/CNT, a cylindrical single-walled CNT with 10nmOD X 9.2 nm ID X 50nm length is embedded in 20nm X 20nm X 100nm square polypropylene unit. The dimension of CNT is in the range of CNT size manufactured by Time Company (China), the purity is above 95%. Perfect bonding is assumed between the phases, and all the phases are considered to be homogeneous, isotropic, and linearly elastic.

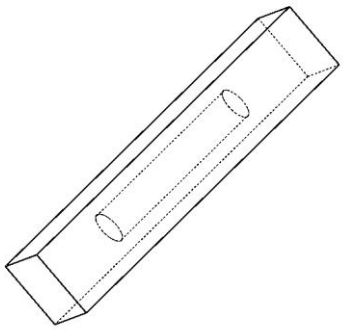

Figure 12. See-through view of PP/CNT model

The material properties used for the RVE include the CNT properties, the properties of PP and CNT/PP contact area. Data input is kept consistent with X.L Chen's, and some

mechanical properties data are from Zamani's research, which can be traced to the for-commercial-use polypropylene supplied from Sabic Company (Saudi Arabia) [4, 13]. Meshing the solid model generates the finite elements, which is crucial for iterative processing in LS-DYNA. To guarantee the accuracy of iteration effectiveness and processing efficiency, four kinds of element size 2nm,3nm, 5nm and 10nm models are designed for optimization. As shown in Figure 12, wherein the matrix has the size of 20x20x100nm, and the CNT has the size of 5nm (outer radius) x4.6nm (inner radius) x50nm length, as shown in Figure 13 and Figure 14.

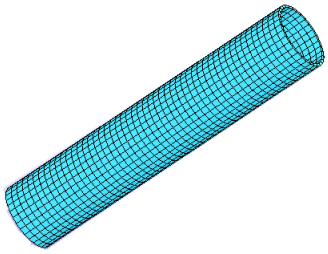

Figure 13. FEA Model polypropylene matrix.

Figure 14. CNT FEA model.

Models with various element size design. Before the mathematical analysis, sensitivity is necessary to improve the accuracy and efficiency. Factors that affect the modeling accuracy can be varied, and element size is one of the significant factors. Additionally, the solver time is directly related to the element size; smaller element size helps to generate a more accurate result; however, it increases the solver time enormously from a few minutes to several hours. Four different models were developed as shown in Figure 15.

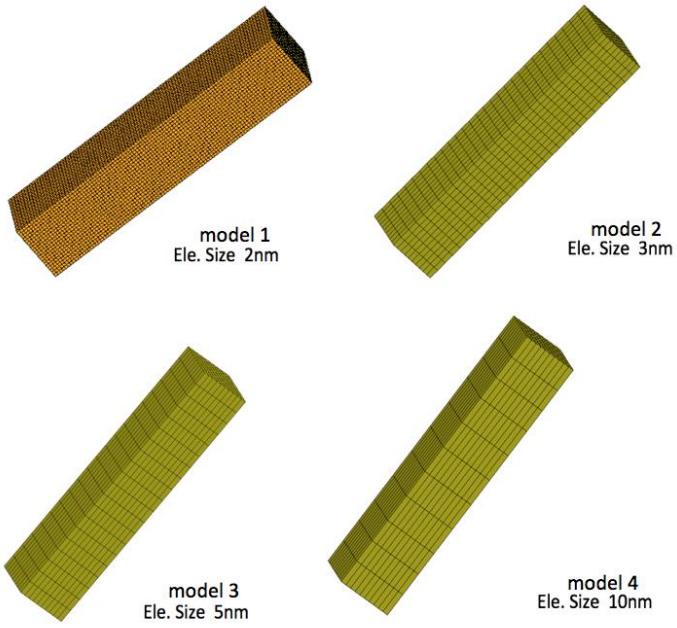

Figure 15. PP/CNT unit with various element size.

It is assumed that CNT and polypropylene units are both homogeneous. Therefore, the property in the X direction is the same with that of Y direction, namely Young's modulus Ex equals to Ey, Poisson's Ratio ν_{zx} equals to ν_{zy}. To validate the eligibility of model, those essential properties of nanocomposites modulus Ratio Ex/Em, Ey/Em, Ez/Em and Poisson's Ratio $\nu_{xy}, \nu_{zx}, \nu_{zy}$ will be compared with X.L Chen's research [13].

Table 2. Mechanical properties of PP/CNT composites material.

Material	Density	Young's Modulus	Poisson's Ratio
CNT	$1g/cm^3$	1000Gpa	0.3
Polypropylene	$1g/cm^3$	100Gpa	0.3

Micro Modeling

Model design. Despite its low density and nanoscale in size, CNT (Carbon Nanotubes) exhibits excellent high stiffness, resilience, and strength. Its unique atomic configuration and sizeable length-to-diameter ratio attract enormous attention. Both theoretical and experimental research have been conducted to discover the relation between its advancing mechanical properties and microstructure. In M. Buongiorno Nardelli's research, they studied the mechanical and electrical properties of CNT response to the external deformation in computational simulation and found the atomic transformation could be related to CNT high strain conditions [8]. X. L Chen et al. developed several models by embedding various CNT geometry shape in polypropylene matrix to reveal the microstructure of PP/CNT unit [1,5]. Zamani et al. researched CNT reinforced polypropylene (PP) wherein the CNT is 0.75 wt%, 1.0 wt%, and 1.5 wt% nanocomposites through low to high-velocity impact performance experiments followed by computational simulation, they found that 1.0 wt% CNT owns better capability of energy absorption. Much other research on CNT microstructure has been done, such as dispersion of CNT in the polymer, simulation with randomly distributed CNTs without causing contacts between CNTs in the polymer matrix is still a challenge though. Y. J Liu et al. developed a macroscale model wherein the CNTs are same oriented but various in the distance.

To research how different CNTs arrangement direction affects the effective mechanical properties of PP/CNT, a brand-new method is developed in this paper with LS-DYNA. The

representative volume element (RVE) idea is applied to define the contact between CNT and Matrix also make macroscale modeling accessible through microscale unit. To obtain a model in which CNTs are dispersed in the random direction, the dimensions of matrix units are intentionally tailored obeying the rule of mixture, which has been proved its validation. Each RVE in this paper consists of 50 nm x 5 nm cylinder CNT and 50 nm x 40nm x 20nm matrix wherein the CNT and matrix are considered as kinetic plastic materials.

Generally, the nano size of CNT is the major problem in the experiments to research the micro changes in CNT even with high-tech equipment such as SEM and TEM. To build a relationship between micro changes in CNT and global performance, models developed are required to have essential features of CNT and can be applied both to micro and microsimulation.

Since CNT dimension is almost seven magnitudes smaller than the sample size and agglomeration is intentionally ignored, single CNT is considered under tension when impacting on the PP/CNT plate with a bullet. In the microscale modeling part, RVE is employed to build models with various arrangements wherein the CNTs are put in the different direction (Figure 29). The dimension of a whole unit used in the tensile simulation is 200nm x 200nm x 20nm. At the same time of studying the properties with the various arrangement, PP/CNT with different CNT weight percentage is also investigated. The mechanical properties of CNT and polypropylene in the column below as shown in Table 3 are applied in the research and resources from [20], which has been tested under tensile and compression simulation and been verified.

Table 3. Mechanical properties of polypropylene and CNT.

	Young's Modulus (GPa)	Poisson's Ratio	Density(g/cm3)
PP	1.38	0.36	1
CNT	70	0.3	1

According to the tensile and compression simulation result on part 1:

in which

E^t is CNT Young's Modulus

E^m is Matrix Young's Modulus

V^t is the volume percentage of CNT

During the tensile simulation, the force was applied as shown in Figure 16. L is the length of PP/CNT model, and ΔL is the elongation after pulling on both sides in the Y direction.

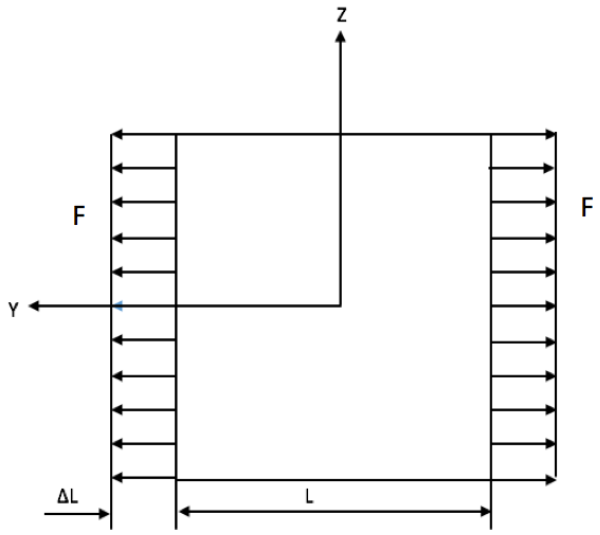

Figure 16. Loads F is applied on both sides of PP/CNT sample model.

Models with various CNT weight percentage and arrangement. In the modeling part, twelve models (Figure 17) with four kinds of CNT weight percentage (0.64%, 0.95%,

1.29%, 1.69%) were conducted with the tensile test, displacement and stress curve were generated by the LS-DYNA system. Taking 0.95 wt% arrangement, for example, Figure 31 demonstrates three different arrangements, which are longitude (Figure 31 model L), both longitude and vertical (Figure 31 model L&V) and vertical (Figure 31 model V).

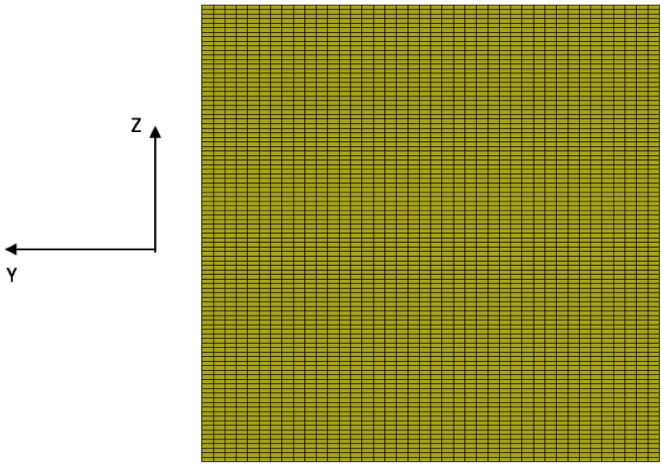

Figure 17. PP/CNT sample model top view.

It is noted that all the models have the same dimension as shown in Figure 17. Changing the CNT amount in the composite material, the weight percentage changes accordingly. Figure 18-21 displays the CNT arrangements, and each weight percentage has three different arrangements referring to Y-axis: L, L&V, V, which means longitude arrangement mixed arrangement and vertical arrangement respectively.

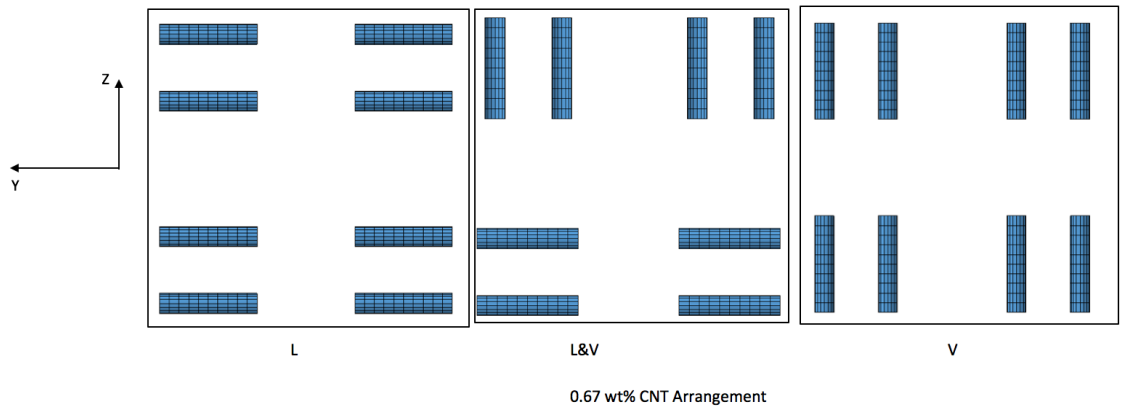

Figure 18. 0.67 wt% CNT arrangements: L, L&V, V.

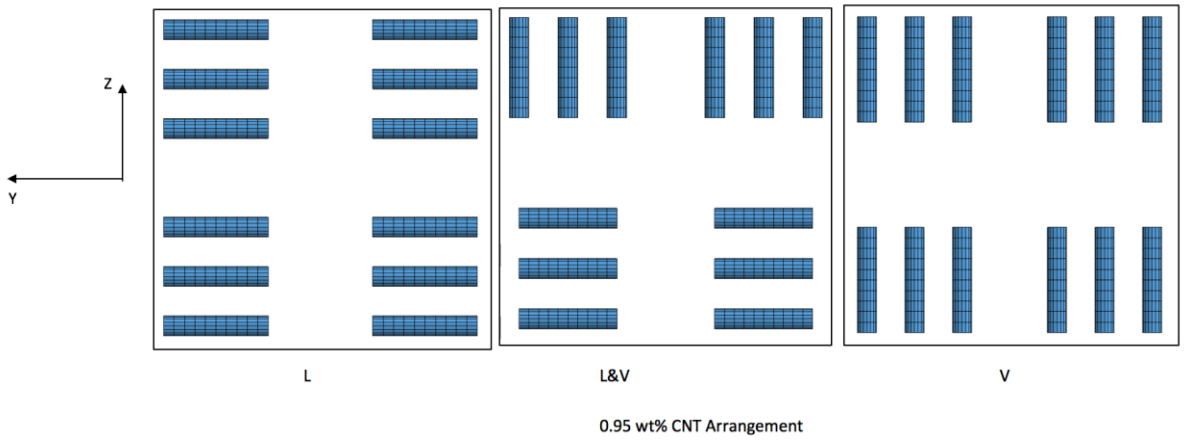

Figure 19. 0.95 wt% CNT arrangements: L, L&V, V.

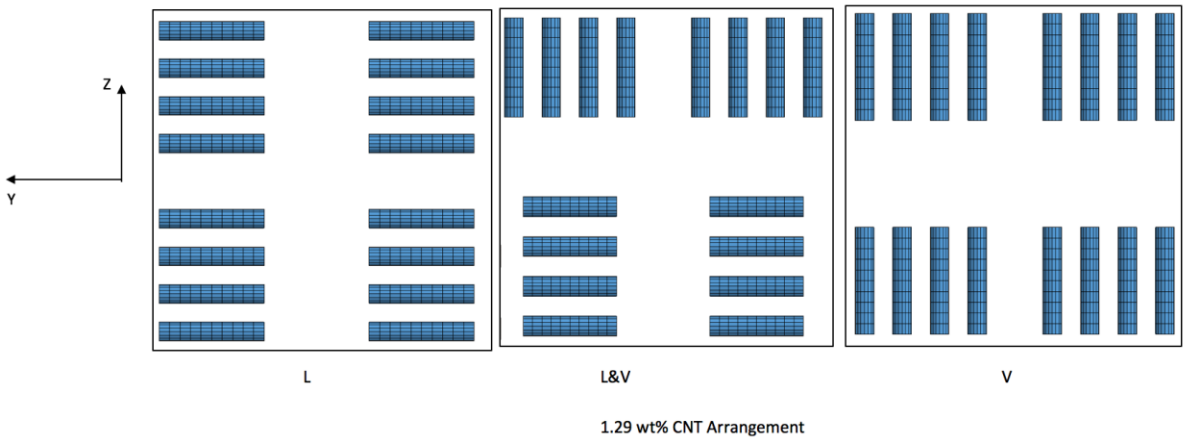

Figure 20. 1.29 wt% CNT arrangements: L, L&V, V.

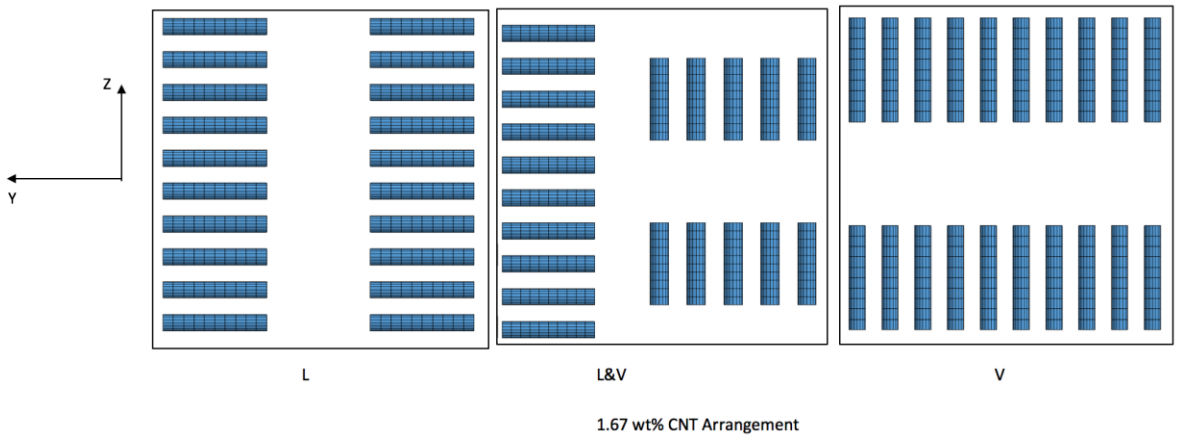

Figure 21. 1.67 wt% CNT arrangements: L, L&V, V.

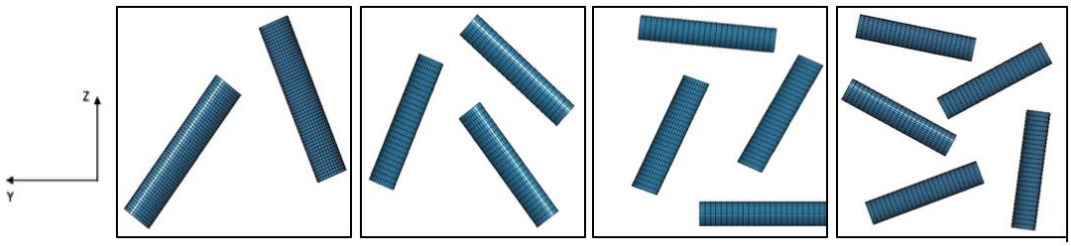

Figure 22. A quarter model of 0.67% (left), 0.95% (second left), 1.29% (third), and 1.67% (right) random CNT arrangements.

Models with various CNF weight percentage and arrangements. The tensile simulation on LS-DYNA reveals the relationship between tensile properties of PP/CNT and CNT arrangements and weight percentage. To develop a successful methodology of Nano/polymer composites tensile simulation which is supposed to be available in the various material with various mechanical constant, the carbon nanofiber reinforced low-density polyethylene composites are selected as the candidate in this paper based on Ahmed Khattab ‘s research[45]. Ahmed Khattab experimentally studied the relationship between the ultimate tensile strength vapor-grown carbon nanofiber (VGCNF) weight percentage, and it is found that the effective Young’s modulus exhibits a linear increase while increasing VGCNF weight percentage, which is shown in Figure 23.

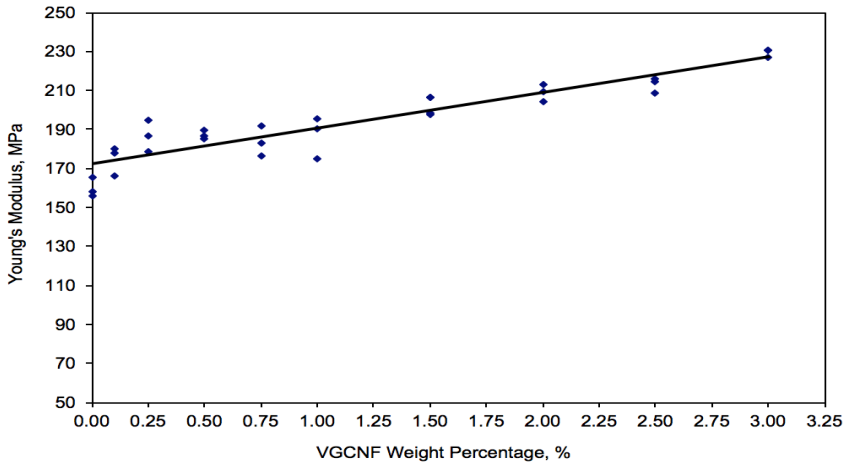

Figure 23. Effective Young's modulus as a function of VGCNF weight percentage [45]**.**

In this paper, models with VGCNF weight percentage of 0.67%, 0.95%, 1.29% and 1.67% are evaluated, it is noted that all the models (Figure 24-27) are in the same arrangements and configuration as shown in Figure 18-21 and the equal loads are employed. The only differences are presented in materials, which is demonstrated in Table 4 [45]

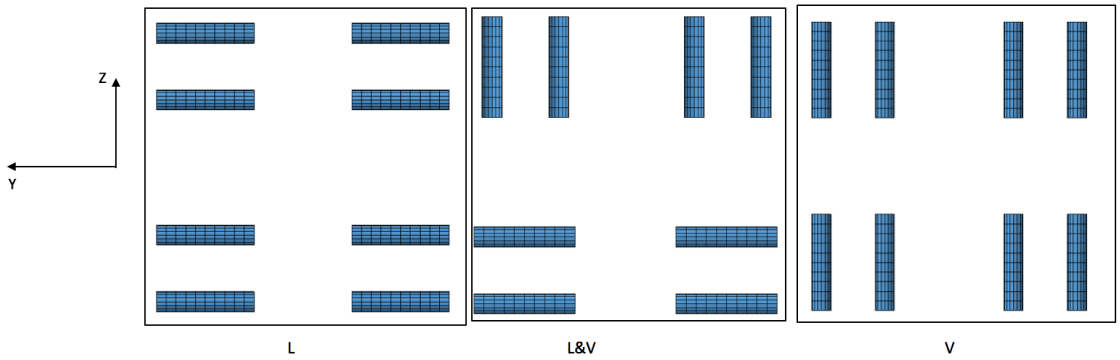

Figure 24. 0.67 wt% CNT arrangements: L, L&V, V.

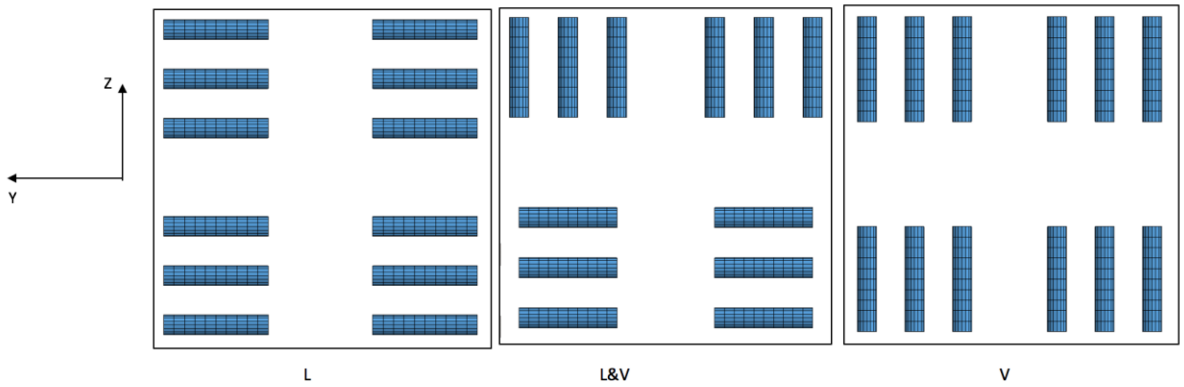

Figure 25. 0.95 wt% CNT arrangements: L, L&V, V.

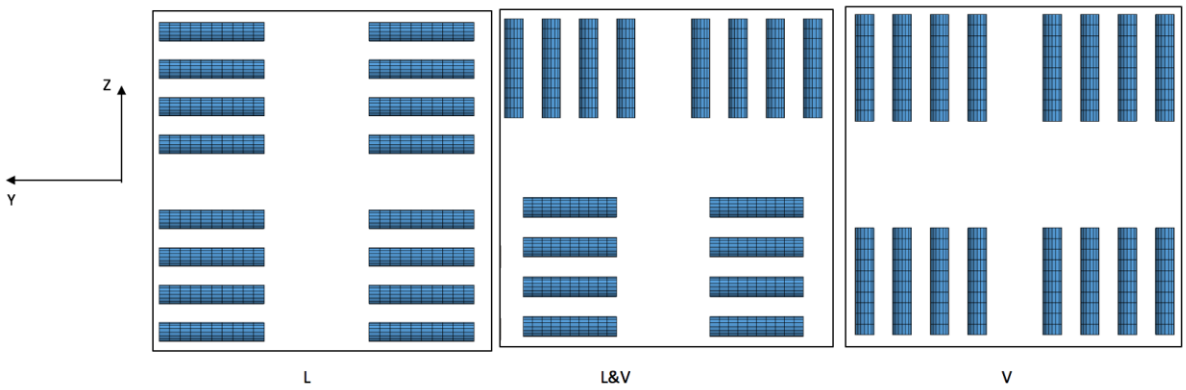

Figure 26. 1.29 wt% CNT arrangements: L, L&V, V.

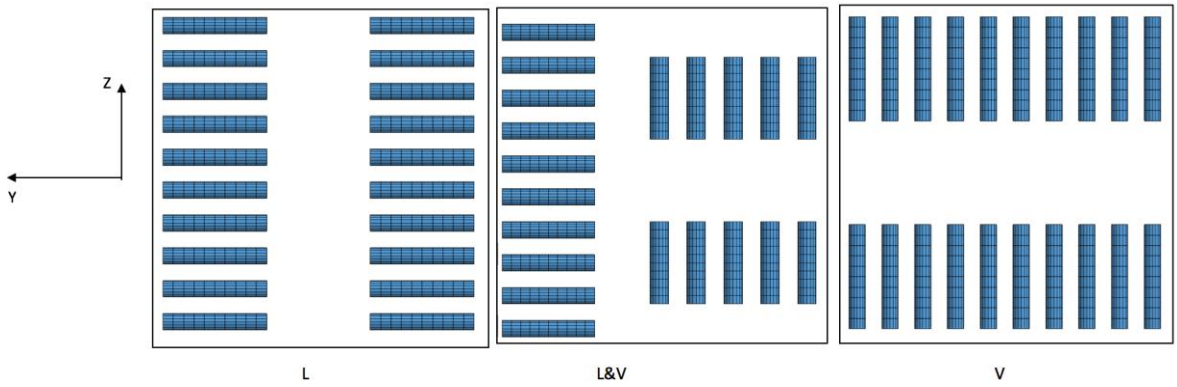

Figure 27. 1.67 wt% CNT arrangements: L, L&V, V.

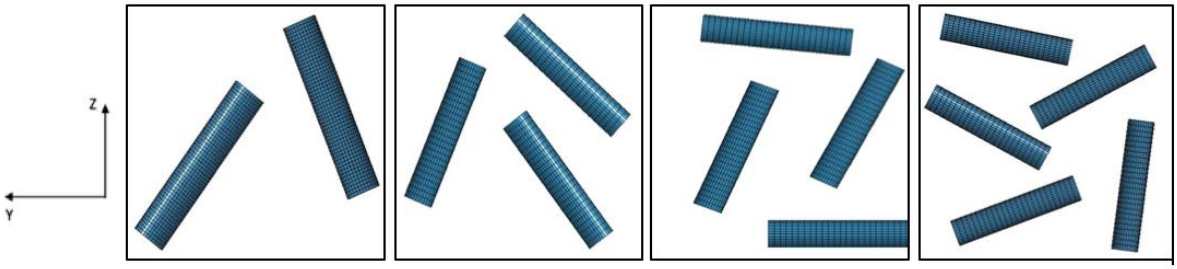

Figure 28. models of VGCNF arranged randomly with various CNF wt.% (0.67%, 0.95%, 1.29% and 1.67%, from left to right).

Table 4. Mechanical properties of polyethylene and VGCNF.

Item	Young's Modulus(GPa)	Poisson's Ratio	Density(g/cm3)
Polyethylene	0.175	0.45	0.92
VGCNF	240	0.25	2

CHAPTER III: MULTISCALE SIMULATION

Nano Simulation

RVE longitude direction tensile simulation. In this load case, the loads (Figure 29) is applied by pulling the RVE in Z-direction with constant velocity, the other end on Z axel keeps fixed. To determine effective Young's modulus at X, Y, Z direction (Ex=Ey) and Poisson's Ratio ν_{zx}, ν_{zy}, a formula that describes the strain-stress relationship is derived as below [13]:

$$\begin{Bmatrix} \varepsilon_x \\ \varepsilon_y \\ \varepsilon_z \end{Bmatrix} = \begin{bmatrix} \frac{1}{Ex} & -\frac{\nu_{xy}}{Ex} & -\frac{\nu_{zx}}{Ez} \\ -\frac{\nu_{xy}}{Ex} & \frac{1}{Ex} & -\frac{\nu_{zx}}{Ez} \\ -\frac{\nu_{zx}}{Ez} & -\frac{\nu_{zx}}{Ez} & \frac{1}{Ez} \end{bmatrix} \begin{Bmatrix} \sigma_x \\ \sigma_y \\ \sigma_z \end{Bmatrix} \qquad \text{Eq. (1)}$$

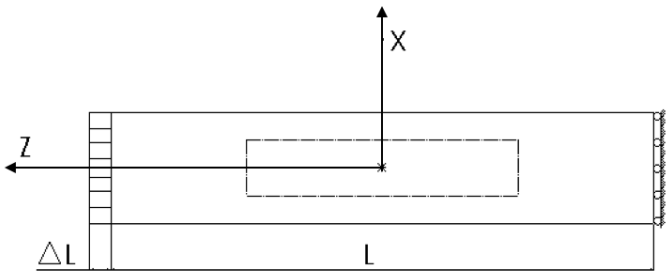

Figure 29. Z-direction loads are employed to stretch the RVE with constant velocity.

According to the simulation result, take some arbitrary nodes (A, B … H) for study. The displacement to time curve is generated from LS-DYNA as shown in Figure 30; A-H are displacement curves from those nodes on RVE model, which reveal the same tendency of x-displacement of each point. An average curve is generated from LS-DYNA (Figure 31), which is based on the scientific calculation by taking data from Figure 30.

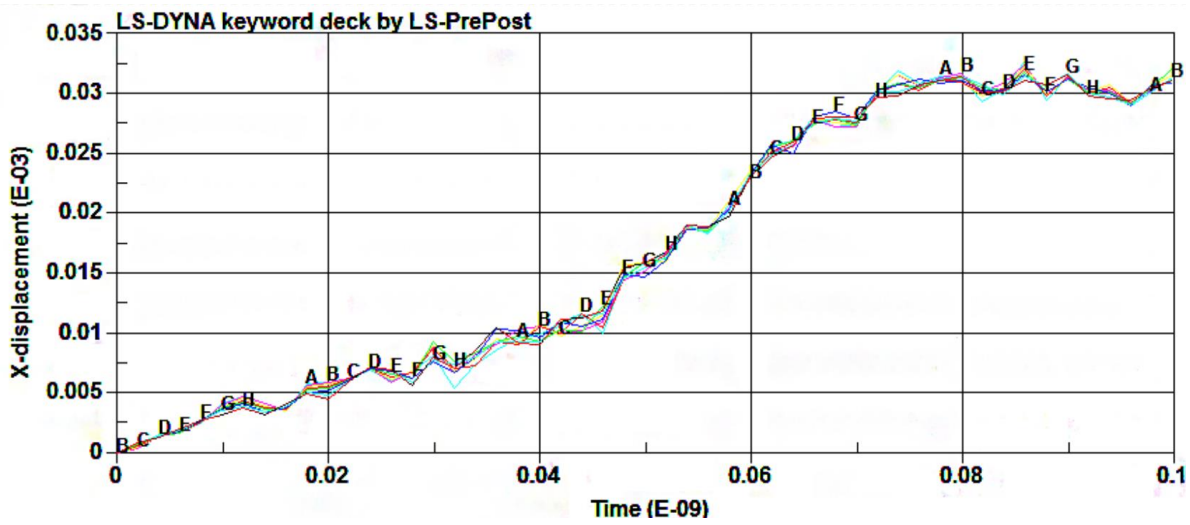

Figure 30. Lateral displacement(um) curves of the different position on RVE when pulling in longitude direction.

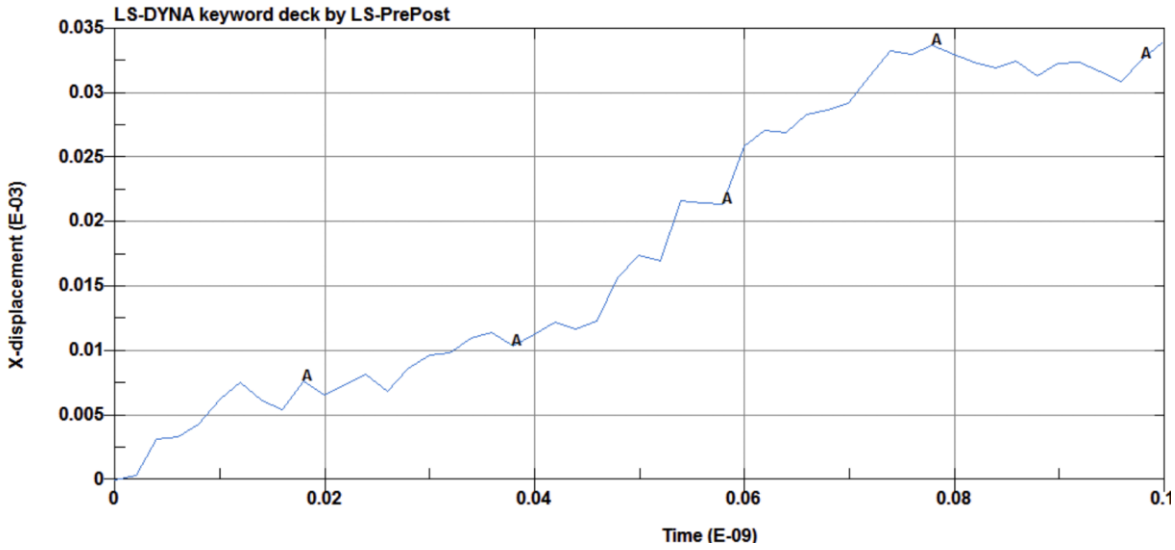

Figure 31. Average lateral displacement (um) curve of the different position on RVE when pulling in longitude direction.

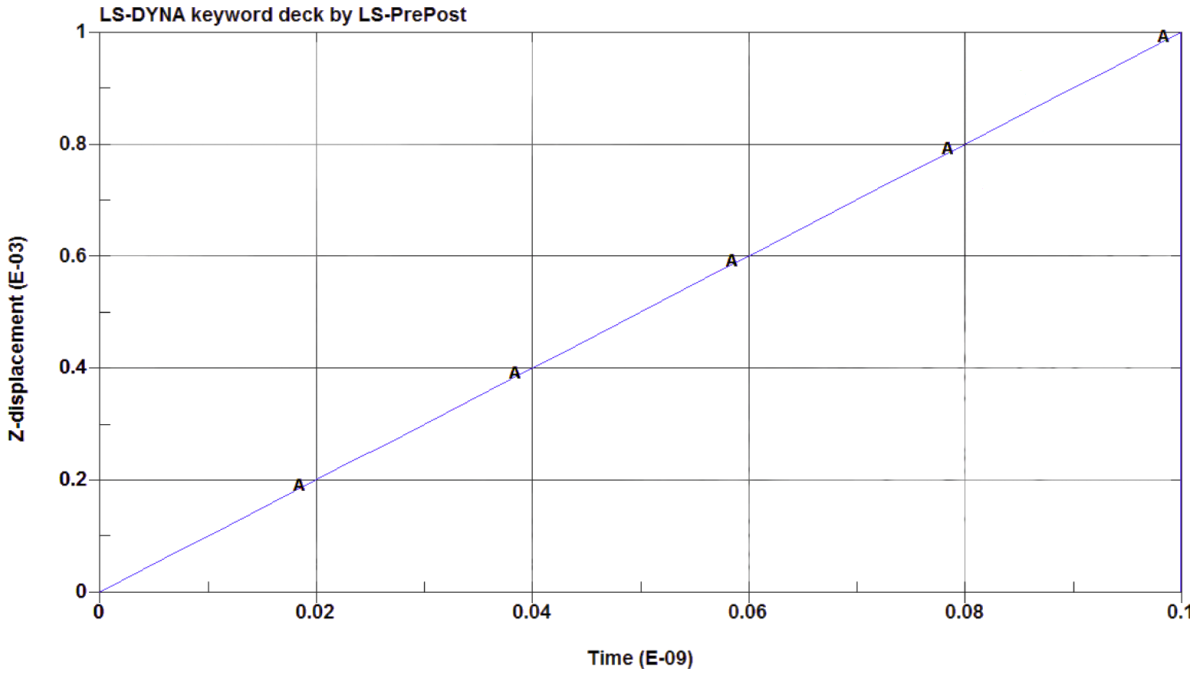

Figure 32. Z-displacement (um) curve RVE when pulling in longitude direction.

In Figure 32, the RVE is stretched in the z-direction with constant velocity and perform in the elastic region; thus, the Z displacement moves absolute linearly. According to elasticity theory, the strain and Poisson's Ratio equations:

$$\varepsilon_x = \frac{\Delta X}{X}, \quad \varepsilon_z = \frac{\Delta Z}{Z} \text{ (X=0.01, Z=0.01)}, \nu_{zx} = \frac{\varepsilon_x}{\varepsilon_z} \qquad \text{Eq. (2)}$$

In this equation, X denotes the length of CNT in the X direction.

For the point on the X, Y lateral surface

$$\sigma_x = \sigma_y = 0$$

X-direction Strain: $\varepsilon_x = \frac{\Delta X}{X} = 100\Delta X$

Z-direction strain: $\varepsilon_z = \frac{\Delta Z}{Z} = 10\Delta Z$

Therefore, the Poisson's Ratio

$$\nu_{zx} = \frac{100\Delta X}{10\Delta Z} \qquad \text{Eq. (3)}$$

Select the first 29 data for statistical analysis with JMP 11 version, the X coordinate is 10ΔZ, and the Y coordinate is 100ΔX from which we can generate the Poisson's Ratio (Figure 33):

$$\nu_{zx} = 0.3082$$

To determine the Young's Modulus Ez, according to Eq. (2)

$$\varepsilon_z = \frac{\Delta Z}{Z}$$

Select the first 29 data for statistical analysis with JMP 11 version, the X coordinate is ε_z, and the Y coordinate is σ_z from which we can generate the Z Young's Modulus:

Ez = 102.467 Gpa

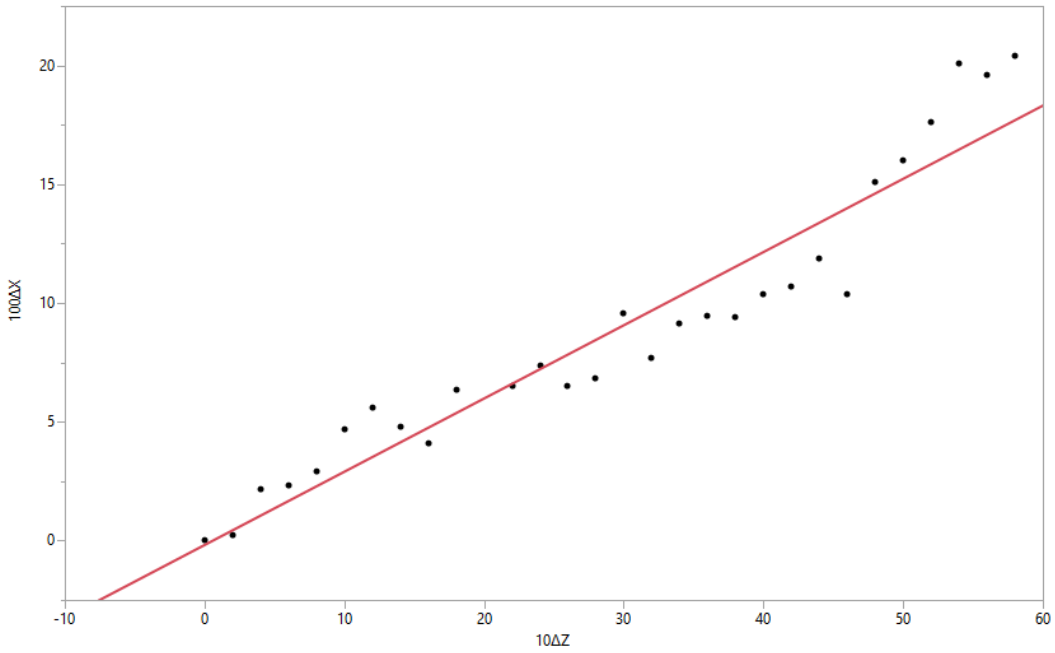

Figure 33. Strain to strain (Poisson's Ratio) $\boldsymbol{\nu_{zx}}$ diagram.

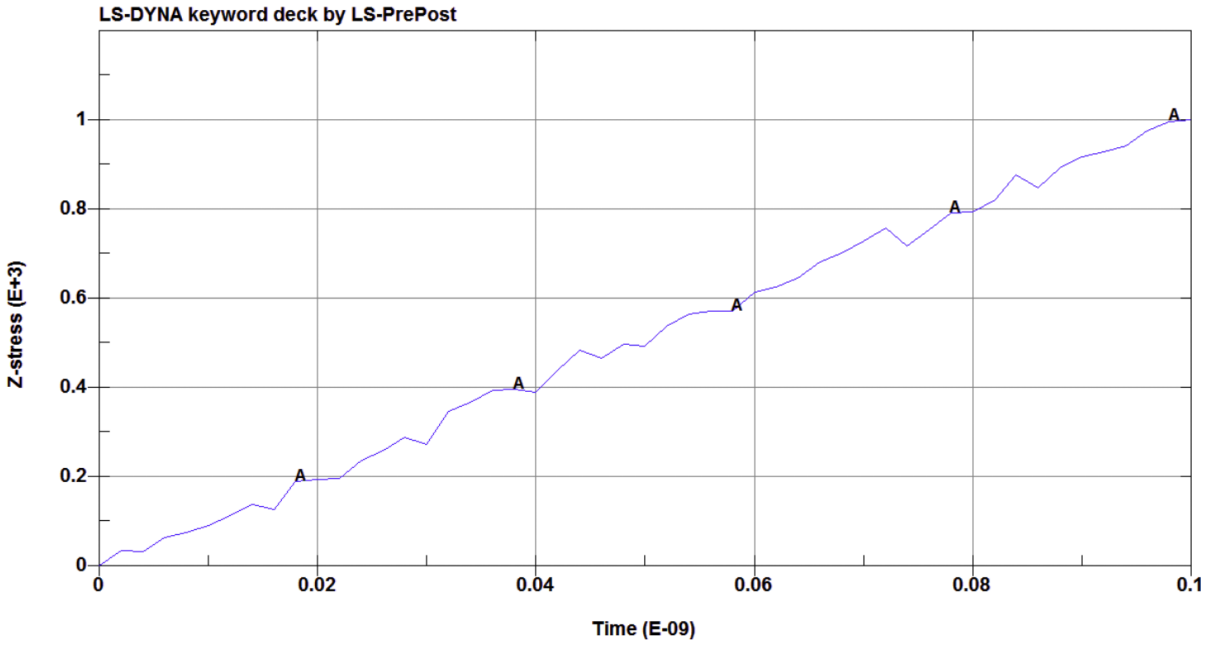

Figure 34. Z-direction stress $\boldsymbol{\sigma_z}$ (Mpa) to time (s)curve under loads.

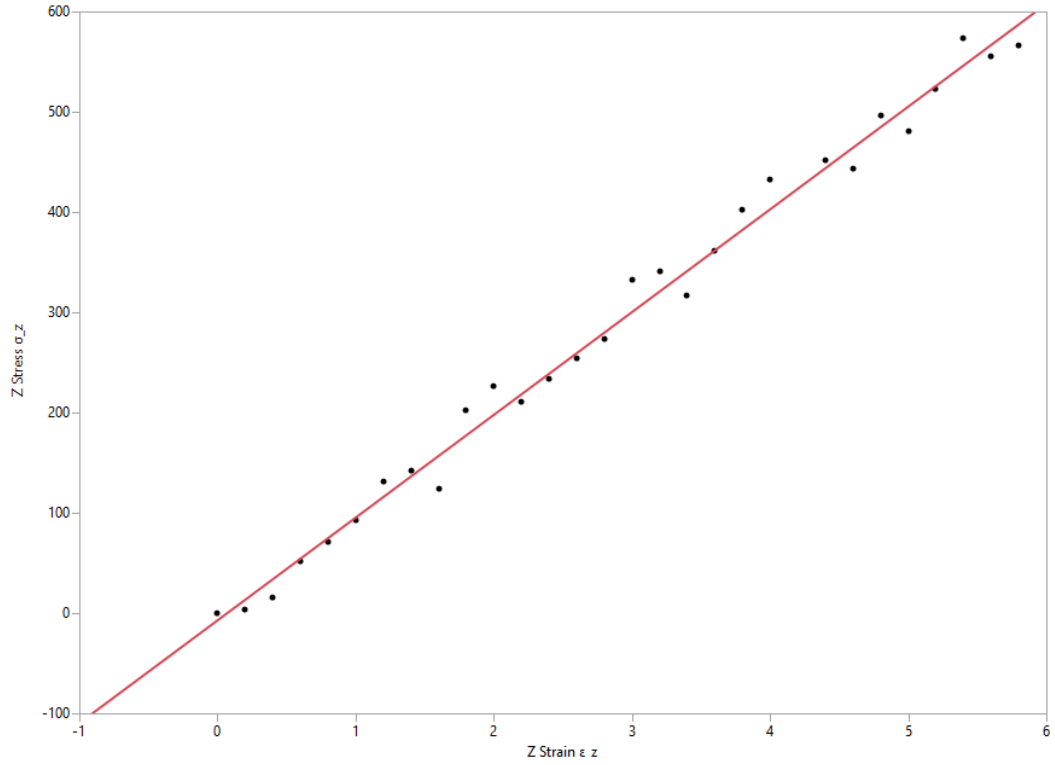

Figure 35. Modified z-directional stress (Mpa) to strain curve (tensile strength).

RVE transversal direction tensile simulation. X-direction tensile simulation, the force applied as shown in Figure 36. According to Eq. (1), when loads applied on X axel, selecting an arbitrary point on the lateral surface.

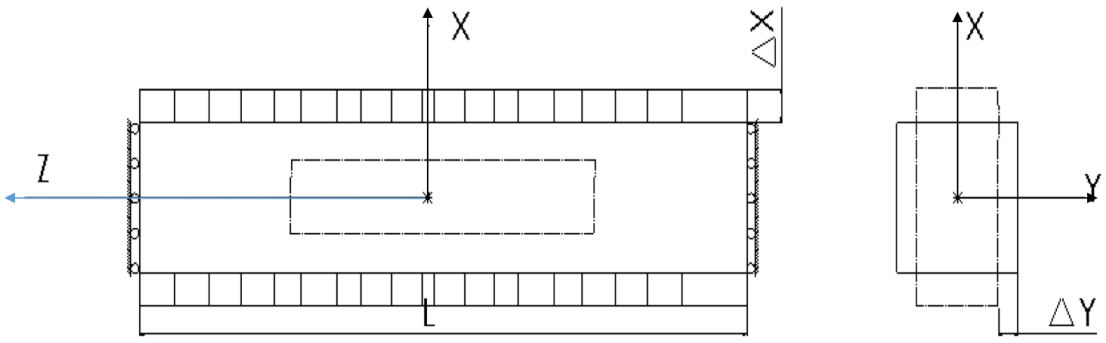

Figure 36. X-direction loads on both sides are employed to stretch the RVE with constant velocity, front view (left) and lateral view (right).

On this surface:

$$\sigma_y = 0,\ \varepsilon_y = \frac{\Delta Y}{Y} = \frac{\Delta Y}{X}$$

From which another equation can be derived:

$$\varepsilon_x = -\left(\frac{\nu_{xy}}{Ey} + \frac{\nu_{zx}\hat{}2}{Ez}\right)\sigma_x = \frac{\Delta X}{X} \qquad \text{Eq. (4)}$$

$$\varepsilon_y = -\left(\frac{1}{Ex} - \frac{\nu_{zx}\hat{}2}{Ez}\right)\sigma_x = \frac{\Delta Y}{X} \qquad \text{Eq. (5)}$$

From Eq. (4). Eq. (5):

$$\frac{1}{Ex} = \frac{1}{Ey} = \frac{\Delta X}{\sigma_x a} + \frac{\nu_{zx}{}^2}{Ez} \qquad \text{Eq. (6)}$$

According to Z-direction tensile simulation from (1)

$$\nu_{zx} = 0.3075$$

$$Ez = 104.75Gpa$$

According to Equation Eq. (3) and Eq. (4), another equation can be derived:

$$\frac{1}{\mathrm{Ex}}=\frac{1}{\mathrm{Ey}}=\frac{\Delta \mathrm{X}}{\sigma_x X}+\frac{{\nu_{zx}}^2}{Ez}$$

In which $\frac{{\nu_{zx}}^2}{Ez}$ and X=0.01 are determined, to get $\frac{1}{\mathrm{Ex}}=\frac{1}{\mathrm{Ey}}$, only $\frac{\Delta \mathrm{X}}{\sigma_x}$ is needed.

Select an arbitrary point on the lateral surface, a curve of ΔX is generated on LS-DYNA (Figure 36). X Stress curve from analysis of the same spot (Figure 37). To guarantee the accuracy of the mathematical calculation, first 29 statistics are selected and analyzed on statistics analysis software JMP 11 version.

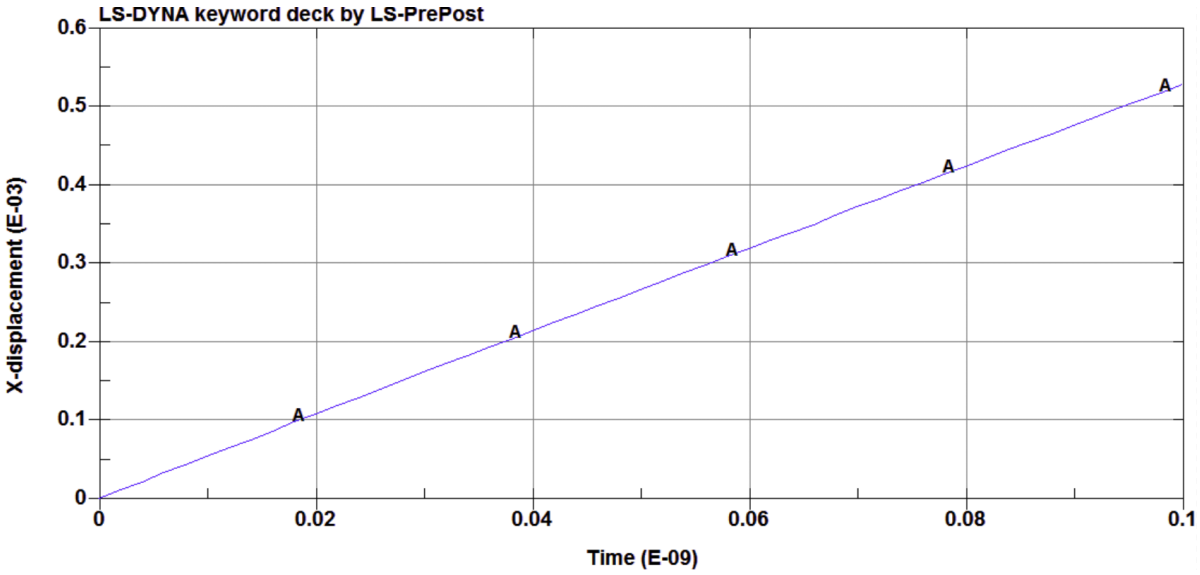

Figure 37. X displacement (um) to time (s) curve when forces are applied to the lateral face (X direction).

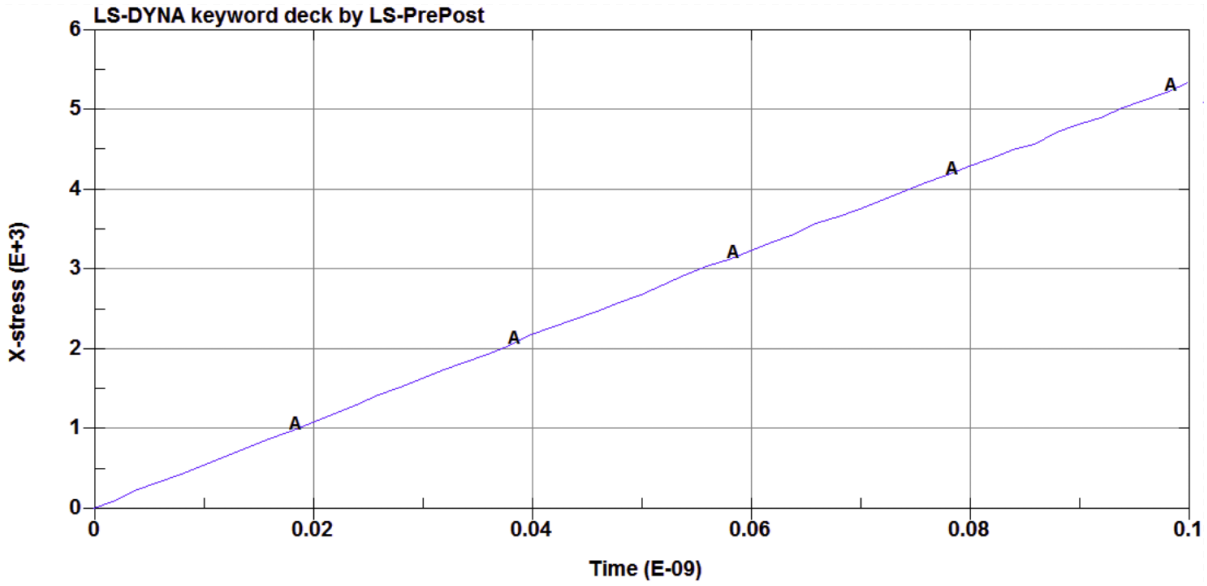

Figure 38. X-direction stress σ_x (Mpa) to time (s) curve when loads are applied along the lateral direction.

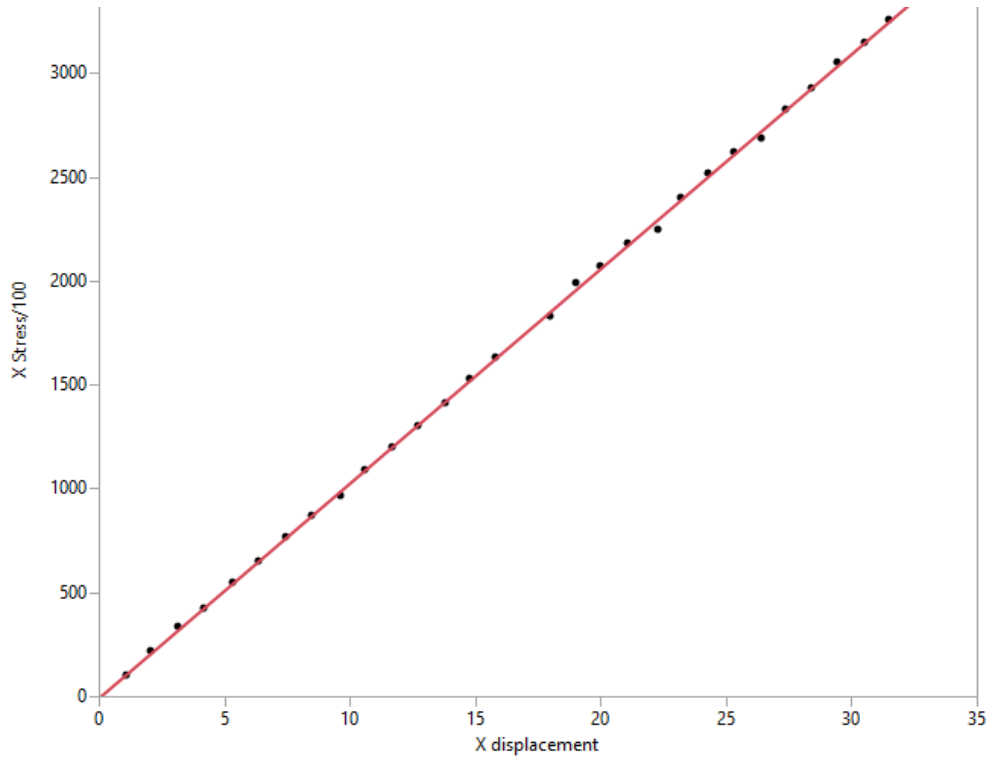

Figure 39. X displacement – X stress curve when loads are applied on lateral direction.

From the curve above, the value can be determined by JMP:

$$\frac{\Delta X}{\sigma_x} = 103.33 \text{ x } 10^{-3}$$

Then Ex = Ey = 95.15 Gpa

According to Eq. (3) and Eq. (4), another equation can be derived:

$$\nu_{xy} = (\frac{\Delta y}{\sigma_x a} + \frac{{\nu_{zx}}^2}{Ez}) / (\frac{\Delta X}{\sigma_x a} + \frac{{\nu_{zx}}^2}{Ez})$$

In this Equation, only $\frac{\Delta y}{\sigma_x}$ needs to be determined. Using the same method above, the curve of Δy as below:

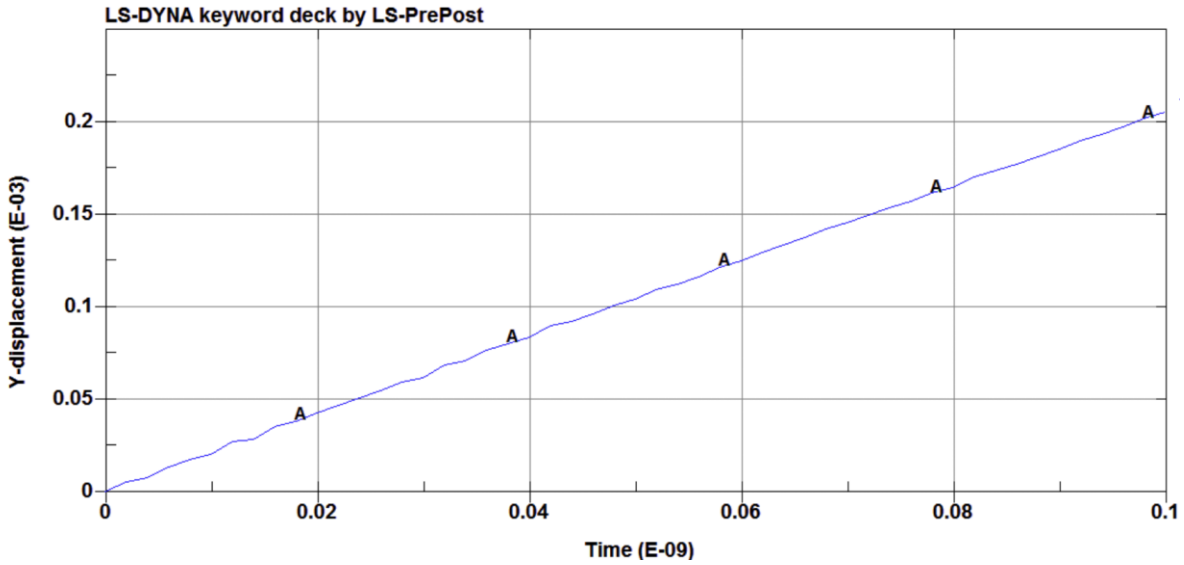

Figure 40. Y displacement (um) to time (s) curve when loads are applied in the lateral direction.

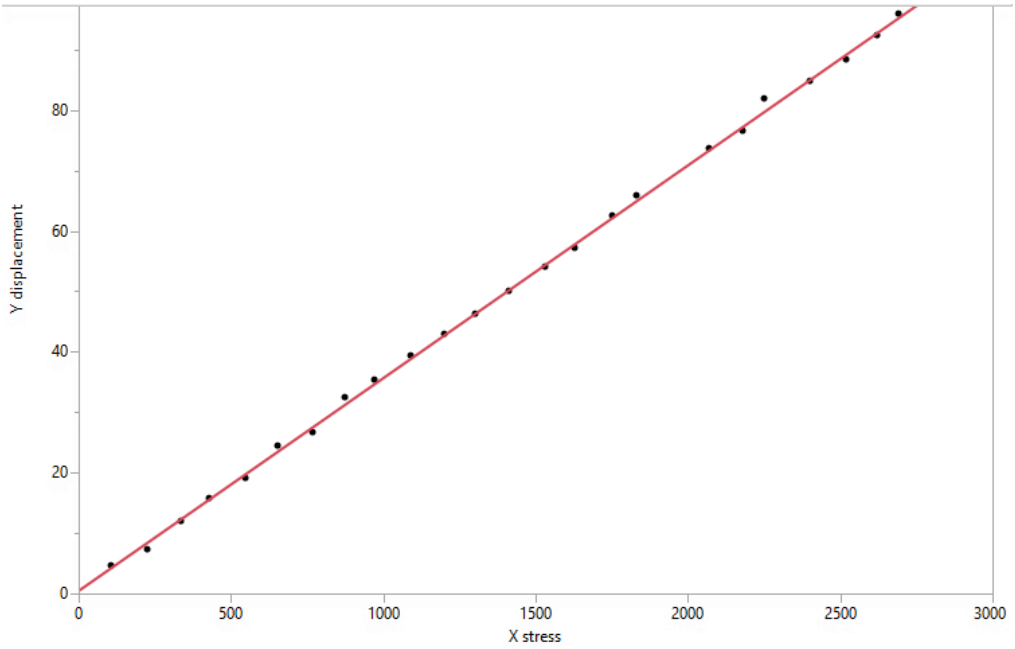

Figure 41. Y displacement (um) to X stress (MPa) curve.

Take data from Figure 40, and Figure 38 for analysis on JMP, the linear relation can be built as demonstrated in Figure 41:

Then the value of $\frac{\Delta y}{\sigma_x}$ generated from software:

$$\frac{\Delta y}{\sigma_x} = 0.0302$$

Therefore: $\nu_{xy} = 0.3218$

And Ex/Em = Ey/Em = 0.9515

Comparison and summary. In order to have a better understanding of how the models perform, Young's modulus and Poisson's ratio are evaluated by comparing with published data. The Young's modulus and Poisson's ratio of nanocomposites models are obtained from modeling and simulation of RVE models on LS-DYNA. All the tensile simulations are conducted in the elastic region in which elasticity theory is confirmed. Compared with the results obtained from published research, which uses ABAQUS[13], the simulation results from LS-DYNA shows very slight difference. As shown in Table 5, when mesh size is 2nm, the difference of Young's modulus between simulation and published data at Z direction is 0.81%, and 1.84% at X and Y direction. The sensitivity study results, as demonstrated in Figure 42, show that when mesh size is 2nm the simulation time is 60 minutes and the time is shortened to 1 minute when the mesh size is 10 nm. However, the shortened time was compromised with decreased accuracy. As it can be seen that when mesh size is at 3nm and 5nm, the accuracy is very close while the simulation time is different. Considering that the time consumed by solving models increases exponentially with the number of units employed, the 5nm mesh is selected as the optimized option.

We can conclude that all the results are consistent with published data. Therefore, on one hand, it is reasonable to consider the RVE model as homogeneous material in nanocomposites simulation. On the other hand, it is also evidential that CNT with atomic structure can also perform well when continuum theory is applied to modeling. Moreover, LS-DYNA as a computational technique is capable of dealing simulation with accuracy and efficiency.

Table 5. The comparison of results of Young's Modulus ratio, Poisson's ratio[13].

FEM model	Ez	ν_{zx}, ν_{zy}	Ex, Ey	ν_{xy}
ABAQUS	103.91	0.3009	93.43	0.3217
LS-DYNA	104.75	0.3075	95.15	0.3218
Difference (%)	0.81%	2.19%	1.84%	0.031%

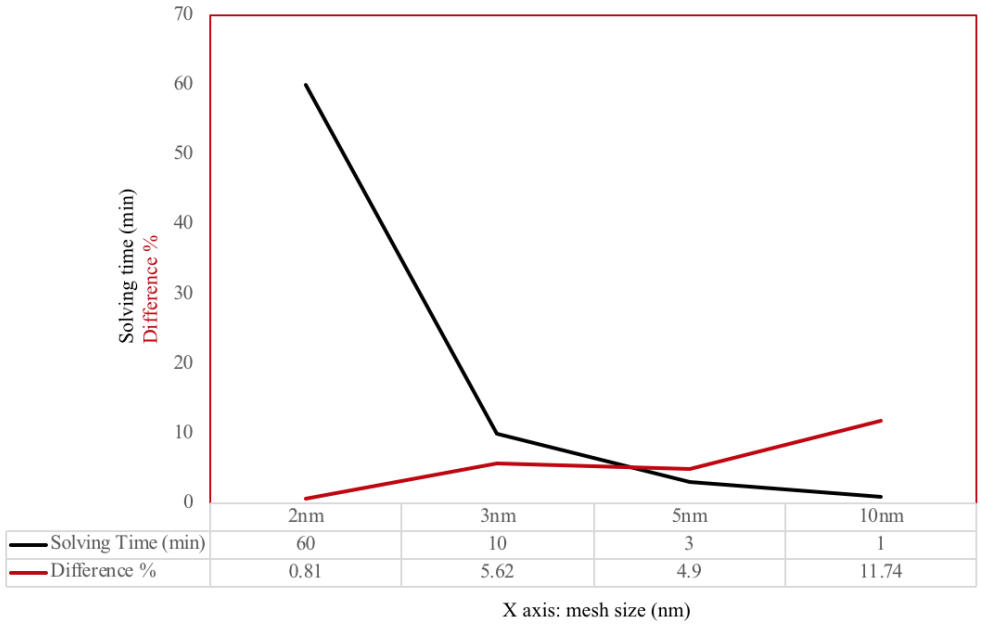

Figure 42. Solving time (min) and difference of Young's modulus compared with published data (103.91 GPa).

Micro and Macro Simulation

PP/CNTs composites with various weight percentage tensile simulation. It is noted that the test happens before the failure mode occurs and the laws of elasticity are obeyed in the mathematical calculation. As described, the loads are applied by pulling the unit in the longitude direction (Figure 16) of CNT with constant velocity. To determine longitude effective Young's modulus, a formula that describes strain-stress relationship [13] is derived as below:

$$\begin{Bmatrix}\varepsilon_x\\ \varepsilon_y\\ \varepsilon_z\end{Bmatrix}=\begin{bmatrix}\frac{1}{Ex} & -\frac{\nu_{xy}}{Ex} & -\frac{\nu_{zx}}{Ez}\\ -\frac{\nu_{xy}}{Ex} & \frac{1}{Ex} & -\frac{\nu_{zx}}{Ez}\\ -\frac{\nu_{zx}}{Ez} & -\frac{\nu_{zx}}{Ez} & \frac{1}{Ez}\end{bmatrix}\begin{Bmatrix}\sigma_x\\ \sigma_y\\ \sigma_z\end{Bmatrix} \quad \text{Eq. (1)}$$

the lateral surface strain and stress are analyzed in this case, and we have

$$\sigma_x = \sigma_z = 0$$

Y-direction strain: $$\varepsilon_Y = \frac{\Delta Y}{Y} = 10\Delta Y \qquad \text{Eq. (2)}$$

Therefore, the tensile modulus in the Y direction

$$E_Y = \frac{\sigma_Y}{\varepsilon_Y} \qquad \text{Eq. (3)}$$

From Eq. (2) Y is already given in the model designing, which is 200nm. ΔY curve is derived from the LS-DYNA; thus, the strain in the Y direction can be obtained. In Eq. (3), the stress in the Y direction can be generated from the system, as shown in Figure 43:

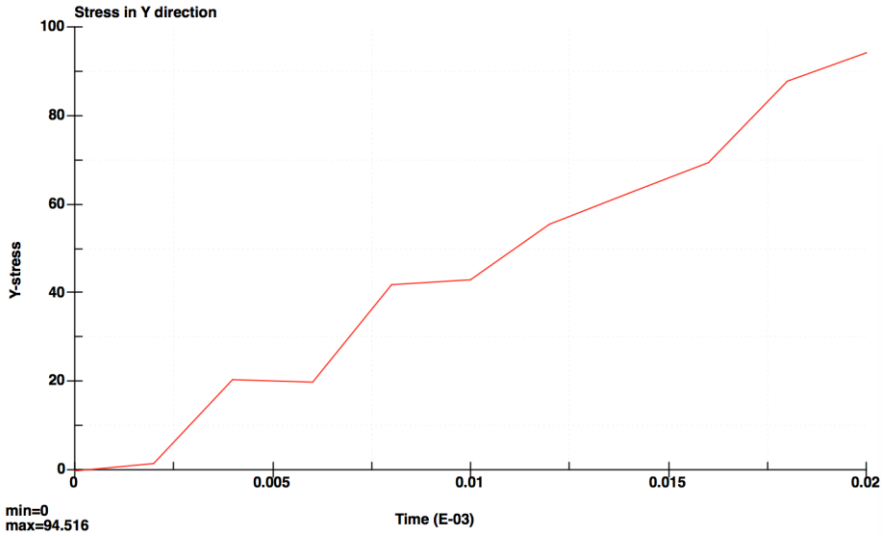

Figure 43. Stress (Mpa) curve of 0.95wt% model L in Y direction.

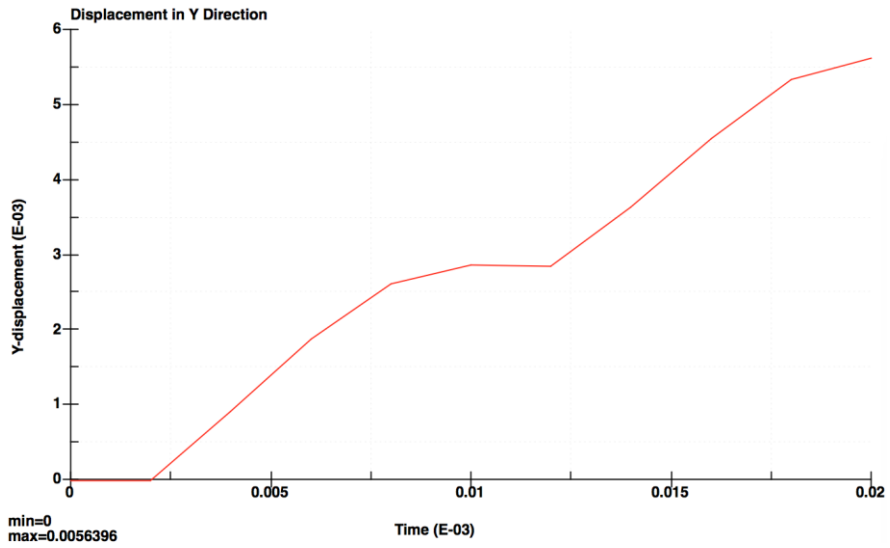

Figure 44. Displacement (um) curve of 0.95wt% model L in Y direction.

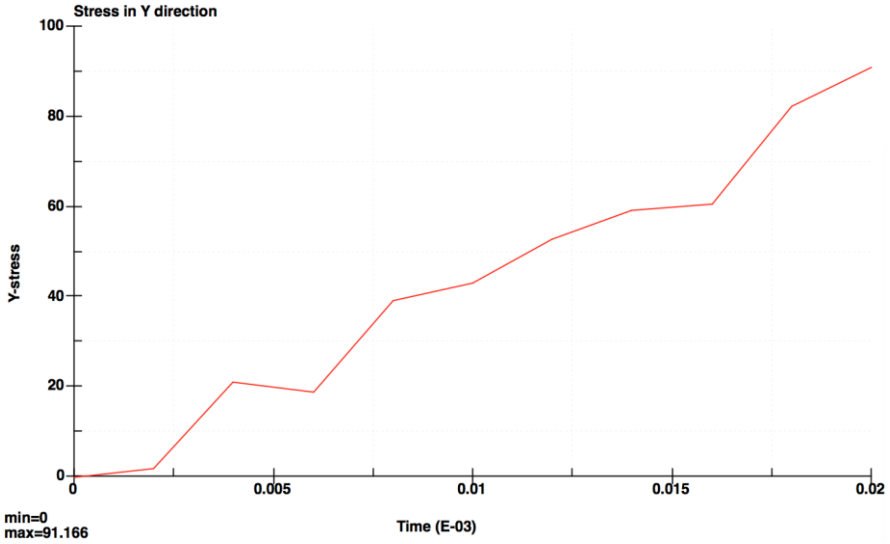

Figure 45. Stress (Mpa) curve of 0.95wt% model L&V in Y direction.

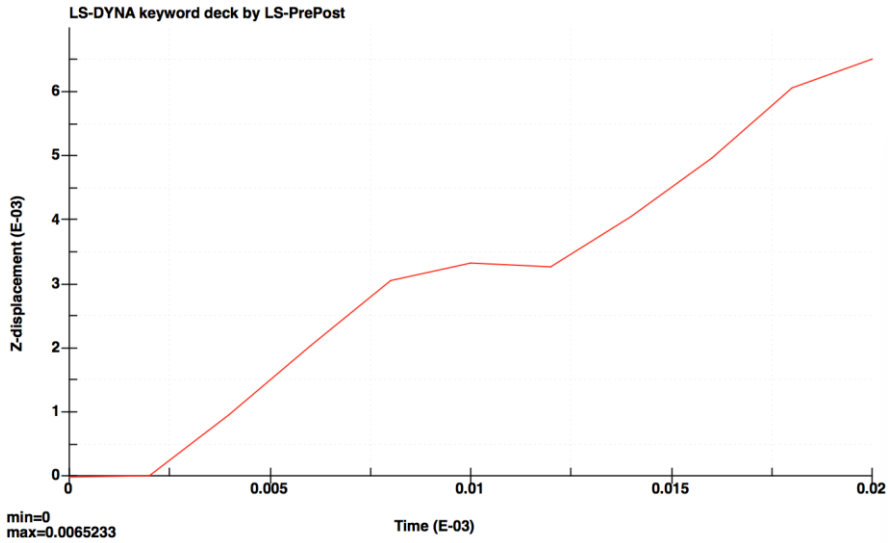

Figure 46. Displacement (um) curve of 0.95wt% model L&V in Y direction.

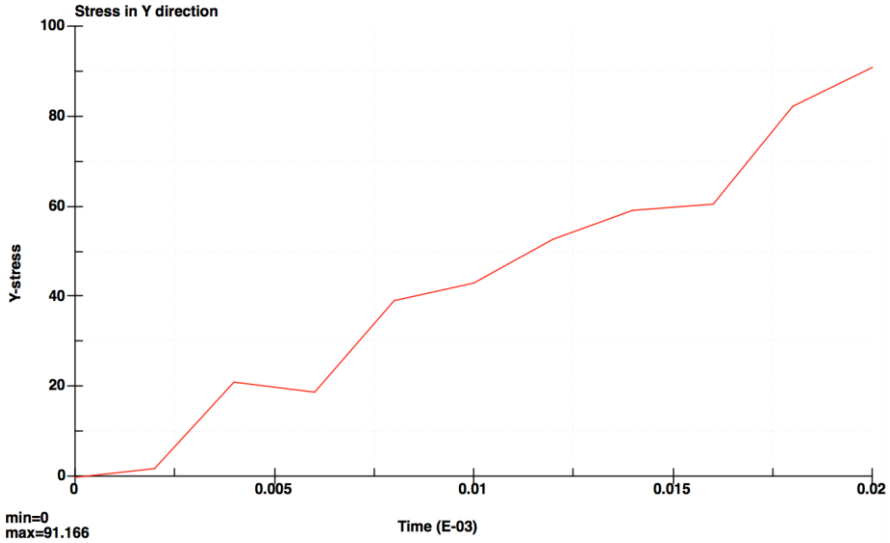

Figure 47. Tensile stress (Mpa) curve of 0.95wt% model V in Y direction.

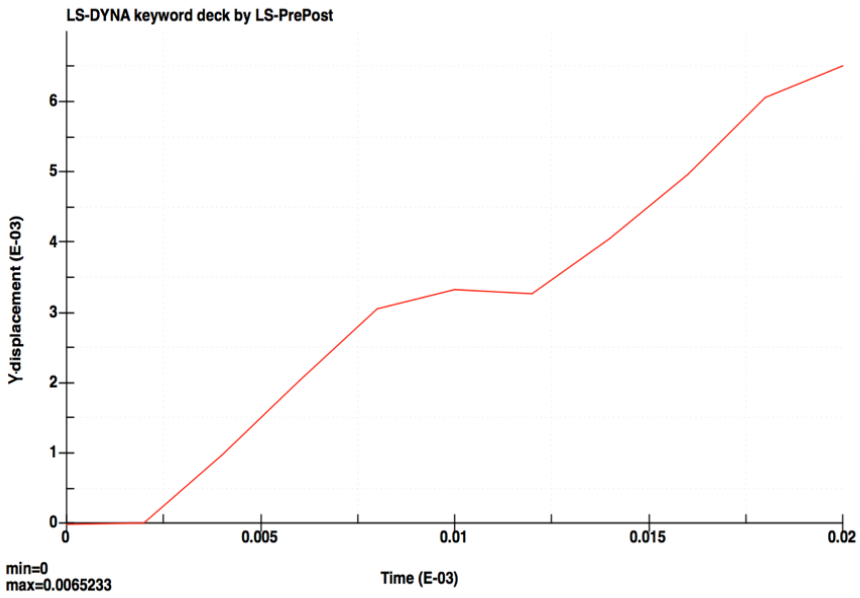

Figure 48. Displacement (um) of 0.95wt% model V in Y-direction.

Data from the models with different CNT arrangements when CNT weight percentage is 0.95% are collected, similarly, displacement and stress curve for other models are generated on LS-DYNA, and all the data is collected in Table 6 from those diagrams [Figure 43-48]. To explicitly demonstrate the effect of the arrangement and weight percentage on the tensile property, a diagram was made as shown in Figure 49. Line L displays the changes of tensile strength by increasing the CNT weight percentage in longitude direction arrangement. The tensile strength of model with CNT arranged in longitude, and the vertical direction is shown in line L&V. The line on the bottom in Figure 50 exhibits the vertical arrangement tensile properties.

Table 6. The tensile strength (Gpa) of PP/CNT model with different CNT weight percentage and arrangements.

CNT Weight Percentage	L	L&V	V	Random
0.67%	1.5	1.39	1.37	1.45
0.95%	1.56	1.41	1.40	1.53
1.29%	1.66	1.44	1.43	1.60
1.67%	1.68	1.52	1.46	1.65

Table 7. Comparison of Young's modulus (Gpa) between experimental data and simulation results with different CNT weight percentage.

Weight Percentage	0.67%	0.95%	1.29%	1.67%
Random (GPa)	185	193	195	200
Experiments (GPa)	187	189	203	209
Difference (%)	1.08	2.07	4.10	4.50

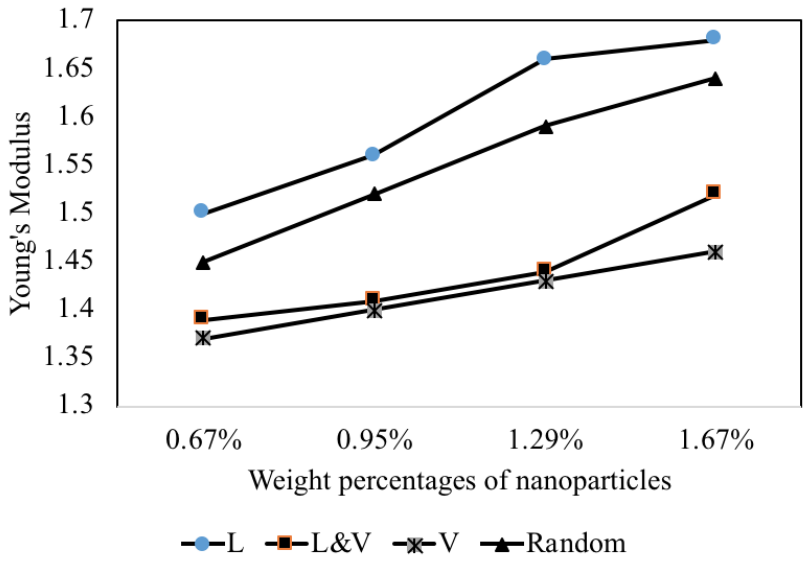

Figure 49. The tensile strength (Gpa) of PP/CNT Model with different CNT Weight Percentage.

Summary for PP/CNTs composites with various weight percentage tensile simulation. As demonstrated in Figure 50, conclusions can be drawn that larger percentage

of CNT arranged in the longitude direction, the tensile strength will be larger accordingly. Examining four different CNT weight percentages, each of them exhibits the same tendency, while 100% CNTs are arranged in the longitude direction, the largest tensile strength can be obtained, the model with 50% CNTs in the longitude direction has the second largest tensile strength. Moreover, increasing the weight percentage from 0.67%, the tensile strength increases correspondingly when the agglomeration is ignored in this simulation since the CNT Young's modulus is much higher than that of the polymer.

PE/CNFs composites with various weight percentage tensile simulation. Stress and strain data are collected on LS-DYNA and analyzed with Eq. (1,7-9), It is shown graphically in Figure 50 that the effective Young's modulus increases linearly while increasing the VGCNF weight percentage.

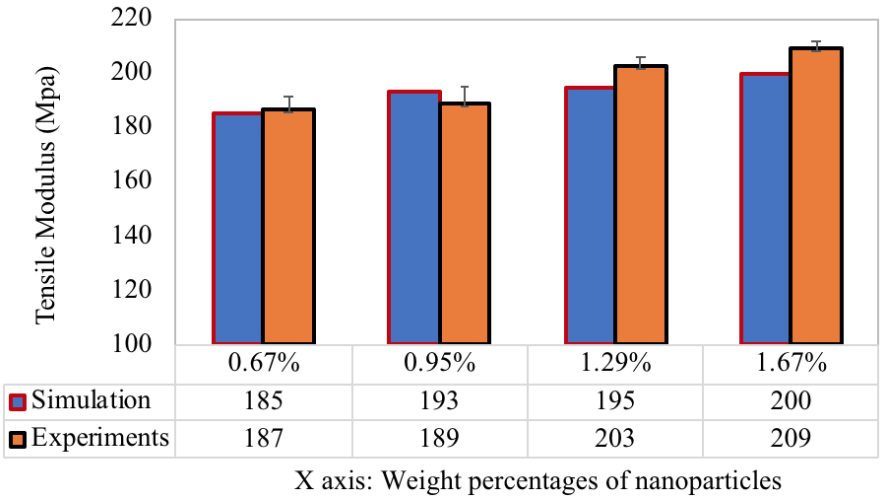

Figure 50. Experimental and computational tensile modulus as a function of VGCNF wt.%

Summary for PE/CNFs composites with various weight percentage tensile simulation. In comparison with the experimental results in Figure 35, Young's modulus of LS-DYNA model not only shows the same increasing tendency but also has a very slight

difference in value at 0.67 wt%, 0.95 wt%, 1.29wt% and 1.67wt% (Figure 50). As known that CNF and CNT are similar in the configuration structure, the difference in physical dimension does not demonstrate the obvious contribution to the tensile property considering that the VGCNF model is still at the nanoscale. The difference as illustrated in Table 7, the smallest difference is 1.08%, and largest difference is 4.5%. It is concluded that the model qualified for CNT reinforced composites also can be extended to VGCNF reinforced composites which have the similar molecule structure. The modeling and simulation in this study can be developed into a methodology for further similar research on CNT or CNF composites.

CHAPTER IV: CONCLUSION AND FUTURE PLAN

Conclusions

The 3-D computational modeling and simulation of tensile properties are conducted on nanoparticles reinforced polymer composite materials at multiscale using finite element analysis method on LS-DYNA. The stress and strain in the models of nanocomposites are analyzed based on the knowledge of elasticity theory, wherein the models are considered as ideal models with perfect interface bonding. Models of the nanocomposites are investigated at three different scales: nanoscale, microscale, and macroscale. At nano and micro scale, the basic unit RVEs used for building model were constructed referring to the dimension and mechanical properties of manufactured single-walled CNT. Then the RVE is examined and validated by comparing simulation results with published data. The mesh size of the RVE is optimized with regards to the simulation accuracy and computational time. Stress and strain data are output form LS-DYNA, and the mathematical calculation on these data show the difference on Young's modulus is small compared with published data. The RVE model is selected with the mesh size of 5nm and simulation error of 4.9 %. In the section of modeling and simulation at micro and macro scale, qualified RVE models are organized to construct models at larger scale. Tensile simulations are conducted on 16 400nm x 400 nm x 20nm Micro models to study nanoparticles orientation and concentration. The results reveal that the nanoparticle direction and weight percentage both impact on the effective mechanical properties. It shows that higher portion of nanoparticles arranged in longitude direction, the better tensile properties nanocomposites have. It also shows that when pulling nanocomposites model in the lateral direction, which is vertical to the nanoparticles orientation, the material has the lowest tensile strength. In addition, increasing the

nanoparticles weight percentage, the tensile strength increases accordingly. When the weight percentage of nanoparticles is 0.67 wt%, the material has the lowest tensile strength, and the material shows the highest tensile strength when nanoparticles weight percentage is 1.67%. In order to validate the adaptability of the microscale model, mechanical properties and physical size of manufactured VGCNF are assigned to the random models, simulation results show that the difference between simulation results and experimental data range from 1.08% to 4.5%. Considering the errors that might appear during the experimental tests, the simulation results are very consistent with experimental results.

Based on the modeling and simulation from nanoscale to macroscale, a generalized and simplified methodology is successfully developed to predict mechanical properties of polymer nanocomposites through simulation. However, this is just the first step towards the macro scale FEA simulations, to have further achievements on the nanoparticles reinforced composites, properties of randomly distributed nanocomposites and nanoparticles agglomerated models still need to be investigated.

Future Plan

This Research made progress on simulation of nanoparticle reinforced composites by developing a methodology that applies to materials with various nano reinforcement. Moreover, the correlation between nanoscale composites and macroscale composites were successfully built. The limitation of this research is that simulation is mainly concentrating on the tensile test on the models, beyond that, it is also worth more exploration on the simulation of projectile with various head shape impacting the composite materials. According to some previous trying of impacting simulation, currently, the most challenging part would be that the impact simulation requires higher computer processing speed. In

addition, LS-DYNA is not capable of building solid models that featured with complex inner structure, a promising alternative to solid model is shell model. Therefore, the future plan would be majorly focusing on the impact of nanoparticles reinforced composites that solid models are represented by shell models.

REFERENCES

1. Hussain, F. "**Polymer-Matrix Nanocomposites, Processing, Manufacturing, and Application: An Overview**" *Journal of Composite Materials* 40, no. 17 (2006): 1511–1575. doi:10.1177/0021998306067321

2. Bikiaris, D. "**Microstructure and Properties of Polypropylene/Carbon Nanotube Nanocomposites**" *Materials* 3, no. 4 (2010): 2884–2946. doi:10.3390/ma3042884

3. Zeng, J., Saltysiak, B., Johnson, W. S., Schiraldi, D. A., and Kumar, S. "**Processing and Properties of Poly(methyl Methacrylate)/carbon Nano Fiber Composites**" *Composites Part B: Engineering* 35, no. 2 (2004): 173–178. doi:10.1016/S1359-8368(03)00051-9

4. Prashantha, K., Soulestin, J., Lacrampe, M. F., Claes, M., Dupin, G., and Krawczak, P. "**Multi-Walled Carbon Nanotube Filled Polypropylene Nanocomposites Based on Masterbatch Route: Improvement of Dispersion and Mechanical Properties through PP-G-MA Addition**" *Express Polymer Letters* 2, no. 10 (2008): 735–745. doi:10.3144/expresspolymlett.2008.87

5. Nicole, L., Laberty-Robert, C., Rozes, L., and Sanchez, C. "**Hybrid Materials Science: A Promised Land for the Integrative Design of Multifunctional Materials**" *Nanoscale* 6, no. 12 (2014): 6267–6292. doi:10.1039/C4NR01788A, Available at http://xlink.rsc.org/?DOI=C4NR01788A

6. Kearns, J. C. and Shambaugh, R. L. "**Polypropylene Fibers Reinforced with Carbon Nanotubes**" *Journal of Applied Polymer Science* 86, no. 8 (2002): 2079–2084. doi:10.1002/app.11160

7. Balazs, A. C., Emrick, T., and Russell, T. P. "**Nanoparticle Polymer Composites: Where Two Small Worlds Meet**" *Science* 314, no. 5802 (2006): 1107–1110. doi:10.1126/science.1130557, Available at http://dx.doi.org/10.1126/science.1130557%5Cnhttp://www.sciencemag.org/content/314/5802/1107.full.pdf

8. Kumar, S. K., Benicewicz, B. C., Vaia, R. A., and Winey, K. I. "**50th Anniversary Perspective: Are Polymer Nanocomposites Practical for Applications?**" *Macromolecules* 50, no. 3 (2017): 714–731. doi:10.1021/acs.macromol.6b02330

9. Ebrahimi, F. "**Nanocomposites New Trends and Developments**" (2012): doi:10.5772/3389

10. Breuer, O. and Sundararaj, U. "**Big Returns from Small Fibers: A Review of Polymer/Carbon Nanotube Composites**" *Polymer Composites* 25, no. 6 (2004): 630–645. doi:10.1002/pc.20058

11. Jordan, J., Jacob, K. I., Tannenbaum, R., Sharaf, M. A., and Jasiuk, I. "**Experimental Trends in Polymer Nanocomposites - A Review**" *Materials Science and Engineering A* 393, no. 1–2 (2005): 1–11. doi:10.1016/j.msea.2004.09.044

12. Mohammadpour, E., Awang, M., Kakooei, S., and Akil, H. M. "**Modeling the Tensile Stress-Strain Response of Carbon Nanotube/polypropylene Nanocomposites Using Nonlinear Representative Volume Element**" *Materials and Design* 58, no. June (2014): 36–42. doi:10.1016/j.matdes.2014.01.007

13. Chen, X. L. and Liu, Y. J. "**Square Representative Volume Elements for Evaluating the Effective Material Properties of Carbon Nanotube-Based Composites**" *Computational Materials Science* 29, no. 1 (2004): 1–11. doi:10.1016/S0927-0256(03)00090-9

14. Figiel, Ł., Dunne, F. P. E., and Buckley, C. P. "**Computational Modelling of Large Deformations in Layered-silicate/PET Nanocomposites near the Glass Transition**" *Modelling and Simulation in Materials Science and Engineering* 18, no. 1 (2010): 15001. doi:10.1088/0965-0393/18/1/015001, Available at http://stacks.iop.org/0965-0393/18/i=1/a=015001?key=crossref.17a8442c927703b1c189d22ab897ada2

15. Zhu, L. and Narh, K. A. "**Numerical Simulation of the Effect of Nanotube Orientation on Tensile Modulus of Carbon-Nanotube-Reinforced Polymer Composites**" *Polymer International* 53, no. 10 (2004): 1461–1466. doi:10.1002/pi.1561

16. Liu, Y., Nishimura, N., and Otani, Y. "**Large-Scale Modeling of Carbon-Nanotube Composites by a Fast Multipole Boundary Element Method**" *Computational Materials Science* 34, no. 2 (2005): 173–187. doi:10.1016/j.commatsci.2004.11.003

17. Zeng, Q. H., Yu, A. B., and Lu, G. Q. "**Multiscale Modeling and Simulation of Polymer Nanocomposites**" *Progress in Polymer Science* 33, no. 2 (2008): 191–269. doi:10.1016/j.progpolymsci.2007.09.002

18. Kaw.Autarr K. "**Mechanics OF Composite Materials**" *Taylor & Francis Group* (2006): 0–473. doi:10.1016/j.fsigen.2011.07.001, Available at http://www.ncbi.nlm.nih.gov/pubmed/21840278

19. Moropoulou, A., Bakolas, A., and Anagnostopoulou, S. "**Composite Materials in Ancient Structures**" *Cement and Concrete Composites* 27, no. 2 (2005): 295–300. doi:10.1016/j.cemconcomp.2004.02.018

20. Callister, W. and Rethwisch, D. "**Materials Science and Engineering: An Introduction**" *Materials Science and Engineering* 94, (2007): doi:10.1016/0025-5416(87)90343-0, Available at http://sinnott.mse.ufl.edu/Syllabus_abet_3010_2007_v02.pdf

21. Wang, R.-M., Zheng, S.-R., and Zheng, Y.-P. "**Introduction to Polymer Matrix Composites**" *Polymer Matrix Composites and Technology* (2011): 1–548. doi:10.1533/9780857092229.1, Available at http://linkinghub.elsevier.com/retrieve/pii/B9780857092212500011

22. Chung, D. D. L. "**Composite Materials: Functional Materials for Modern Technologies**" *Engineering Materials and Processes* 1, (2002): doi:10.1017/CBO9781107415324.004

23. R.E. Shalin. "**Polymer Matrix Composites**" *Chapman & Hall* (1995): doi:10.1007/978-0-387-74365-3, Available at https://www.princeton.edu/~ota/disk2/1988/8801/880106.PDF

24. Bhuiyan, M. A., Pucha, R. V., Worthy, J., Karevan, M., and Kalaitzidou, K. "**Defining the Lower and Upper Limit of the Effective Modulus of CNT/polypropylene Composites through Integration of Modeling and Experiments**" *Composite Structures* 95, (2013): 80–87. doi:10.1016/j.compstruct.2012.06.025, Available at http://dx.doi.org/10.1016/j.compstruct.2012.06.025

25. Sun, L., Gibson, R. F., Gordaninejad, F., and Suhr, J. "**Energy Absorption Capability of Nanocomposites: A Review**" *Composites Science and Technology* 69, no. 14 (2009): 2392–2409. doi:10.1016/j.compscitech.2009.06.020, Available at http://dx.doi.org/10.1016/j.compscitech.2009.06.020

26. Nilakantan, G., Keefe, M., Bogetti, T. A., Adkinson, R., and Gillespie, J. W. "**On the Finite Element Analysis of Woven Fabric Impact Using Multiscale Modeling Techniques**" *International Journal of Solids and Structures* 47, no. 17 (2010): 2300–2315. doi:10.1016/j.ijsolstr.2010.04.029, Available at http://dx.doi.org/10.1016/j.ijsolstr.2010.04.029

27. Gusev, A. A. "**Representative Volume Element Size for Elastic Composites: A Numerical Study**" *Journal of the Mechanics and Physics of Solids* 45, no. 9 (1997): 1449–1459. doi:10.1016/S0022-5096(97)00016-1, Available at http://www.sciencedirect.com/science/article/pii/S0022509697000161

28. Hbaieb, K., Wang, Q. X., Chia, Y. H. J., and Cotterell, B. "**Modelling Stiffness of Polymer/Clay Nanocomposites**" *Polymer* 48, no. 3 (2007): 901–909. doi:10.1016/j.polymer.2006.11.062

29. Haggenmueller, R., Gommans, H. H., Rinzler, A. G., Fischer, J. E., and Winey, K. I. "**Aligned Single-Wall Carbon Nanotubes in Composites by Melt Processing Methods**" *Chemical Physics Letters* 330, no. 3–4 (2000): 219–225. doi:10.1016/S0009-2614(00)01013-7

30. Liu, Y. . and Chen, X. . "**Evaluations of the Effective Material Properties of Carbon Nanotube-Based Composites Using a Nanoscale Representative Volume Element**" *Mechanics of Materials* 35, no. 1–2 (2003): 69–81. doi:10.1016/S0167-6636(02)00200-4

31. Zhang, H. and Zhang, Z. "**Impact Behaviour of Polypropylene Filled with Multi-Walled Carbon Nanotubes**" *European Polymer Journal* 43, no. 8 (2007): 3197–3207. doi:10.1016/j.eurpolymj.2007.05.010

32. Du, J. H., Bai, J., and Cheng, H. M. "**The Present Status and Key Problems of Carbon Nanotube-Based Polymer Composites**" *Express Polymer Letters* 1, no. 5 (2007): 253–273. doi:10.3144/expresspolymlett.2007.39

33. Hutton, D. V. "**Fundamentals of Finite Element Analysis**" *Textbook (Important)* (2004): 494. doi:10.1017/CBO9781107415324.004, Available at http://books.google.com/books?id=rQSiQgAACAAJ&pgis=1

34. Frogley, M. D., Ravich, D., and Wagner, H. D. "**Mechanical Properties of Carbon Nanoparticle-Reinforced Elastomers**" *Composites Science and Technology* 63, no. 11 (2003): 1647–1654. doi:10.1016/S0266-3538(03)00066-6

35. Finegan, I. C., Tibbetts, G. G., and Gibson, R. F. "**Modeling and Characterization of Damping in Carbon Nanofiber/polypropylene Composites**" *Composites Science and Technology* 63, no. 11 (2003): 1629–1635. doi:10.1016/S0266-3538(03)00054-X

36. Zare, Y. "**Determination of Polymer-Nanoparticles Interfacial Adhesion and Its Role in Shape Memory Behavior of Shape Memory Polymer Nanocomposites**" *International Journal of Adhesion and Adhesives* 54, (2014): 67–71. doi:10.1016/j.ijadhadh.2014.05.004, Available at http://dx.doi.org/10.1016/j.ijadhadh.2014.05.004

37. Zare, Y. "**Study of Nanoparticles Aggregation/agglomeration in Polymer Particulate Nanocomposites by Mechanical Properties**" *Composites Part A: Applied Science and Manufacturing* 84, (2016): 158–164. doi:10.1016/j.compositesa.2016.01.020, Available at http://dx.doi.org/10.1016/j.compositesa.2016.01.020

38. Mortazavi, B., Bardon, J., and Ahzi, S. "**Interphase Effect on the Elastic and Thermal Conductivity Response of Polymer Nanocomposite Materials: 3D Finite Element Study**" *Computational Materials Science* 69, (2013): 100–106. doi:10.1016/j.commatsci.2012.11.035

39. Pontefisso, A., Zappalorto, M., and Quaresimin, M. "**An Efficient RVE Formulation for the Analysis of the Elastic Properties of Spherical Nanoparticle Reinforced Polymers**" *Computational Materials Science* 96, no. PA (2015): 319–326. doi:10.1016/j.commatsci.2014.09.030, Available at http://dx.doi.org/10.1016/j.commatsci.2014.09.030

40. Marcadon, V., Brown, D., Hervé, E., Mélé, P., Albérola, N. D., and Zaoui, A. "**Confrontation between Molecular Dynamics and Micromechanical Approaches to Investigate Particle Size Effects on the Mechanical Behaviour of Polymer Nanocomposites**" *Computational Materials Science* 79, (2013): 495–505. doi:10.1016/j.commatsci.2013.07.002, Available at http://dx.doi.org/10.1016/j.commatsci.2013.07.002

41. Zare, Y. "**Development of Halpin-Tsai Model for Polymer Nanocomposites Assuming Interphase Properties and Nanofiller Size**" *Polymer Testing* 51, (2016): 69–73. doi:10.1016/j.polymertesting.2016.02.010, Available at http://dx.doi.org/10.1016/j.polymertesting.2016.02.010

42. Quaresimin, M., Schulte, K., Zappalorto, M., and Chandrasekaran, S. "**Toughening Mechanisms in Polymer Nanocomposites: From Experiments to Modelling**" *Composites Science and Technology* 123, (2016): 187–204. doi:10.1016/j.compscitech.2015.11.027, Available at http://dx.doi.org/10.1016/j.compscitech.2015.11.027

43. Jajam, K. C. and Tippur, H. V. "**Quasi-Static and Dynamic Fracture Behavior of Particulate Polymer Composites: A Study of Nano- vs. Micro-Size Filler and**

Loading-Rate Effects" *Composites Part B: Engineering* 43, no. 8 (2012): 3467–3481. doi:10.1016/j.compositesb.2012.01.042, Available at http://dx.doi.org/10.1016/j.compositesb.2012.01.042

44. Gitman, I. M., Askes, H., and Sluys, L. J. "**Representative Volume: Existence and Size Determination**" *Engineering Fracture Mechanics* 74, no. 16 (2007): 2518–2534. doi:10.1016/j.engfracmech.2006.12.021

45. Khattab, A., Liu, C., Chirdon, W., and Hebert, C. "**Mechanical and Thermal Characterization of Carbon Nanofiber Reinforced Low-Density Polyethylene Composites**" *Journal of Thermoplastic Composite Materials* 26, no. 7 (2013): 954–967. doi:10.1177/0892705711432361, Available at http://jtc.sagepub.com/content/26/7/954.abstract

APPENDIX

```
$# LS-DYNA Keyword file   created by LS-PrePost 4.0 -   28-Jan-13      (19:00)
$# Created on Jul-14-20      15 (22:0       7:28)
*KEYWORD
*TITLE
$# title
LS-DYNA keyword deck by  LS-PrePost
*CONTROL_ACCURACY
$#     osu       inn       pidosu
1       3         0
*CONTROL_ENERGY
$#    hgen      rwen      slnten   rylen
2       2         2         2
*CONTROL_TERMINATION
$#  endtim    endcyc    dtmin   endeng endmas
1.0000E-10        0       0         0         0
*CONTROL_TIMESTEP
$#  dtinit    tssfac       isdo     tslimt   dt2ms  lctm     erode    ms1st
```

1.0000E-12 0.9000000 0 0 0 0 0

$# dt2msf dt2mslc imscl unused unused rmscl

0.000 0 0 0

*DATABASE_ELOUT

$# dt binary lcur ioopt option1 option2 option3 option4

2.0000E-12 0 0 1 0 0 0 0

*DATABASE_GLSTAT

$# dt binary lcur ioopt

2.0000E-12 0 0 1

*DATABASE_MATSUM

$# dt binary lcur ioopt

2.0000E-12 0 0 1

*DATABASE_NCFORC

$# dt binary lcur ioopt

2.0000E-12 0 0 1

*DATABASE_RCFORC

$# dt binary lcur ioopt

2.0000E-12 0 0 1

*DATABASE_BINARY_D3PLOT

$# dt lcdt beam npltc psetid

2.0000E-12 0 0 0 0

$# ioopt

0

*BOUNDARY_PRESCRIBED_MO TION_SET _ID

$# id heading

0MOVE

$# nsid dof vad lcid sf vid death birth

3 1 2 1 1 1 0.00E+00 0

*BOUNDARY_SPC_SET

$# nsid cid dofx dofy dofz dofrx dofry dofrz

1 0 1 1 1 1 1 1

*SET_NODE_LIST_TITLE

NODESET(SPC) 1

$# sid da1 da2 da3 da4 solver

1 0.000 0 0 0.000M ECH

Xiao, Xiaoguang. Bachelor of Science, Wuhan University of Technology, 2013; Master of Science, University of Louisiana at Lafayette, Spring 2018
Major: Engineering, Mechanical Engineering concentration
Title of Thesis: Multi-scale Modeling and Simulation of Nanoparticles Reinforced Polymer Composites
Thesis Director: Dr. Ahmed Khattab
Pages in Thesis: 88; Words in Abstract: 234

ABSTRACT

Over the years, the properties of nanoparticle-reinforced composites have been investigated regarding how the overall mechanical properties of the composites can be influenced by weight percentages, particle size, and types of reinforcement. The current advanced material processing technology allows people to obtain customized materials. However, making composite materials is usually costly and time-demanding, and some composite waste does not easily degrade. This computational study on composites provides a promising solution to these problems. In this research, a methodology of studying nanoparticle-reinforced polymer composites is developed, which allows the simulation of mechanical properties with multiscale computational approach. First, an RVE model of general nanoparticle-reinforced composites is constructed at nanoscale, and a computational study is made to examine the tensile behavior of the RVE on LS-DYNA. Second, a sensitivity study is conducted to optimize the mesh size with regards to simulation accuracy and computational time. Also, the model is validated by comparing the results from simulation with published data. Third, RVE models are applied to develop multiple models at microscale featured with various nanoparticles reinforcement dosages and orientation. In the end, data from tensile experiments on VGCNF are utilized to verify the models. It is found that using RVE models shortened the simulation times significantly while maintaining relatively high accuracy. Also, those models can be extensively applied to simulate various

nanocomposites at multiple scales, which will fill the gap of simulation at between nanoscale and microscale.

BIOGRAPHICAL SKETCH

Xiaoguang Xiao was born in Hubei Province, China, on March 8, 1990. He obtained his Bachelor of Science in Mechanical Engineering from Wuhan University of Technology in China in July 2013. He joined the University of Louisiana at Lafayette in January 2015 to pursue a Master of Science in Engineering with a concentration in Mechanical Engineering. He completed his M.S. degree in Spring of 2018.